Cell Tissue Res
DOI 10.1007/s00441-007-0439-x

REGULAR ARTICLE

Association of TIMP-2 with extracellular matrix exposed to mechanical stress and its co-distribution with periostin during mouse mandible development

Nagako Yoshiba · Kunihiko Yoshiba · Akihiro Hosoya · Masahiro Saito · Takamasa Yokoi · Takashi Okiji · Norio Amizuka · Hidehiro Ozawa

Received: 21 November 2006 / Accepted: 27 April 2007

Abstract Matrix remodeling is regulated by matrix metalloproteinases (MMPs) and tissue inhibitors of metalloproteinases (TIMPs). Periostin, originally identified in a mouse osteoblastic library, plays a role in cell adhesion and migration and in mechanical stress-induced matrix remodeling. In this study, we analyzed and compared the distribution patterns of TIMP-2 and periostin during mouse mandible development. Immunohistochemical staining for TIMP-2 and periostin was carried out on serial cryosections obtained from mice at embryonic days 13–16, postnatal day 2 (P2), P35, and 12 weeks of age. TIMP-2 and periostin exhibited a strikingly similar protein distribution during mandible development. From bud to early bell stages of molars, TIMP-2 and periostin were highly expressed on the lingual and anterior sides of the basement membrane and on the adjacent jaw mesenchyme. In pre- and postnatal incisors, the basement membrane of the apical loop and dental follicle was immunostained for TIMP-2 and periostin. At postnatal stages, TIMP-2 and periostin were prominently confined to the extracellular matrix (ECM) of gingival tissues, periodontal ligaments, and tendons (all recipients of mechanical strain). However, periostin was solely detected in the lower portion of the inner root sheath of hair follicles. Gingiva of P2 cultured in anti-TIMP-2 antibody-conditioned medium showed markedly reduced staining of periostin. We suggest that TIMP-2 and periostin are co-distributed on ECM exposed to mechanical forces and coordinately function as ECM modulators.

Keywords TIMP-2 · Periostin · Extracellular matrix · Tooth development · Periodontal tissue · Mouse

This work was supported by the Japanese Ministry of Education, Culture, Sports, Science, and Technology and by Niigata University Research Projects.

N. Yoshiba (✉) · K. Yoshiba · T. Okiji
Division of Cariology, Operative Dentistry and Endodontics, Department of Oral Health Science, Niigata University Graduate School of Medical and Dental Sciences,
5274 Gakkocho-dori 2-bancho,
Niigata 951-8514, Japan
e-mail: nagako@dent.niigata-u.ac.jp

A. Hosoya
Department of Oral Histology, Matsumoto Dental University, Shiojiri, Japan

M. Saito
Department of Biochemistry, Osaka University Graduate School of Dentistry, Osaka, Japan

T. Yokoi
Department of Medicine, Division of Operative Dentistry and Endodontics, Kanagawa Dental College, Kanagawa, Japan

N. Amizuka
Center for Transdisciplinary Research, Niigata University, Niigata, Japan

H. Ozawa
Institute for Dental Science, Matsumoto Dental University, Shiojiri, Japan

Introduction

Remodeling of the extracellular matrix (ECM) plays a critical role in normal development and in physiological and pathological processes. Matrix metalloproteinases (MMPs) are zinc-dependent proteases capable of degrading all ECM constituents. The activity of these proteases is tightly regulated by actions of tissue inhibitors of metal-

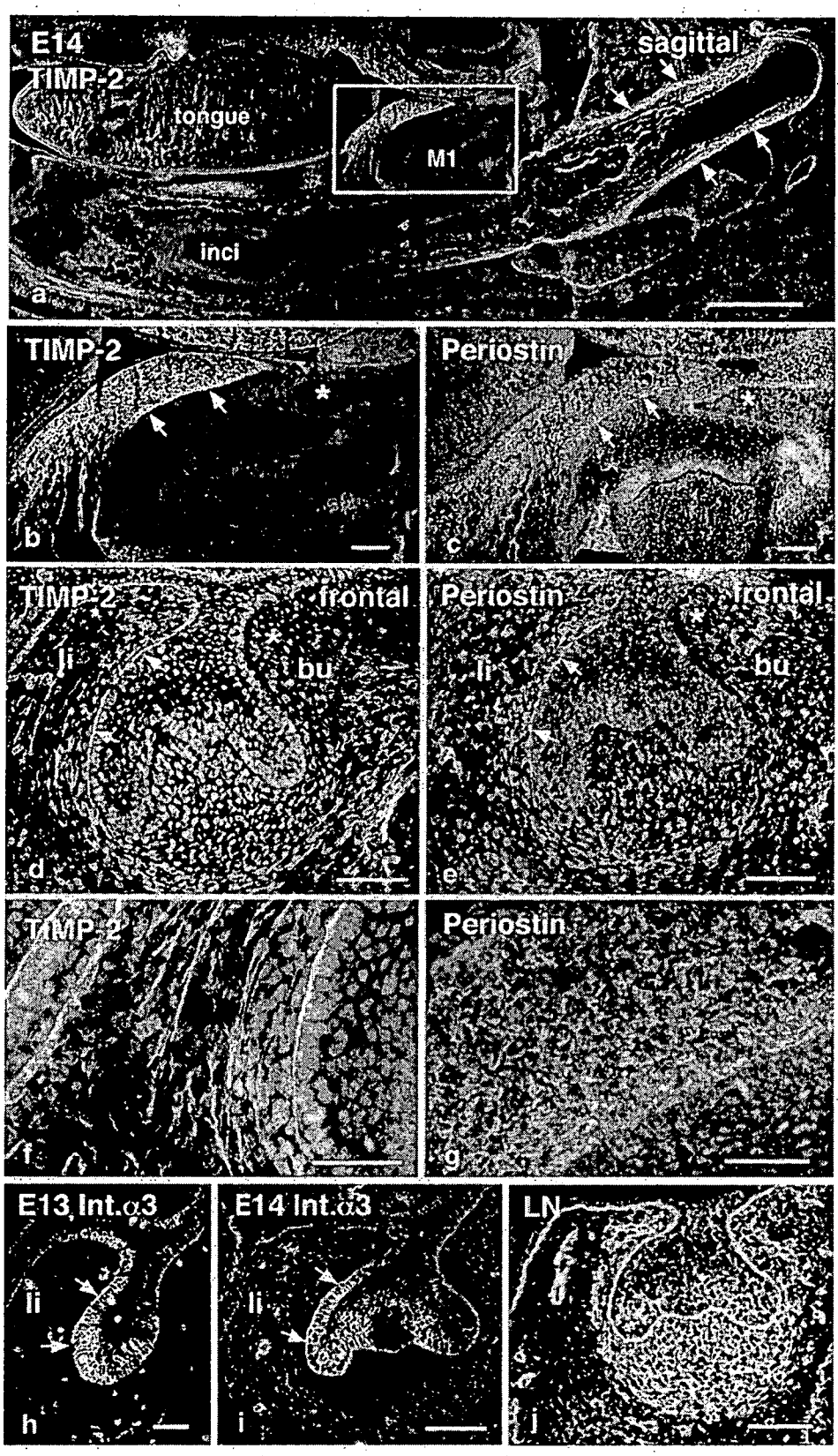
E14
TIMP-2
tongue
M1
sagittal
inci
a
TIMP-2
b
Periostin
c
TIMP-2
frontal
li
bu
d
Periostin
frontal
li
bu
e
TIMP-2
f
Periostin
g
E13 Int.α3
li
h
E14 Int.α3
li
i
LN
j

◀ **Fig. 1** Immunohistochemical detection of TIMP-2 and periostin in the mandible at embryonic day (E) 14. **a** Low-power image of a sagittal section of mandible immunostained for TIMP-2. TIMP-2 is restricted to the mandible (*arrows* expression of TIMP-2 on the tendon of Ramus of the mandible, *M1* first molar, *inci* incisor). **b** Higher magnification of *boxed area* in **a**. TIMP-2 is present in the jaw mesenchyme at the anterior part of the molar and along the adjacent basement membrane (*arrows*). In contrast to the anterior region, the posterior part is devoid of TIMP-2 (*asterisk*). **c** Serial section of **b** immunostained for periostin. The tissue distribution of periostin is similar to that of TIMP-2. **d**, **e** Serial frontal sections showing TIMP-2 and periostin expression, respectively. Both proteins are present along the dental basement membrane on the lingual side (*li*) of the molar (*arrows*) and in the adjacent jaw mesenchyme. In contrast, the buccal side (*bu*) is devoid of both proteins (*asterisks*). **f** High-power image of **d** showing that TIMP-2 is associated with ECM. **g** High-power image of **c** demonstrating that periostin lies on the cell surface. **h**, **i** Frontal sections of the molar tooth germ at E13 (**h**) and E14 (**i**) immunostained for integrin α3 (*Int.α3*). Integrin α3 is strongly detected on the lingual side (*li*) of the dental epithelium (*arrows*). **j** Basement membrane of molar germ at E14 labeled for laminin (*LN*) on the frontal section. *Bars* 500 μm (**a**), 100 μm (**b–e**, **h–j**), 50 μm (**f**, **g**)

loproteinases (TIMPs), which are also secreted into the ECM. Efficiencies of MMP inhibition vary among TIMPs, and the balance between MMPs and TIMPs determines the most significant proteolytic events in tissue remodeling. TIMP-2 is ubiquitously expressed as a soluble form in almost every tissue and inhibits various MMPs. TIMP-2 can act as a major inhibitor of membrane-type-1 MMP (MT1-MMP), which is the membrane-anchored-type MMP, and MMP-2. On the other hand, TIMP-2 is essential for the activation of proMMP-2 by MT1-MMP, and excess TIMP-2 completely inhibits the activity of MT1-MMP and activation of proMMP-2 (Seiki 2002). MT1-MMP can digest fibrillar collagen types I, II, and III, and other ECM components including denatured collagen (gelatin), proteoglycans, fibronectin, laminin 1, and vitronectin (Ohuchi et al. 1997). MT1-MMP also activates proMMP-13 (collagenase 13; Knauper et al. 1996a), which degrades fibrillar collagen types I, II, and III (Knauper et al. 1996b). MMP-2 degrades gelatin and collagen types I and IV. In type I collagen-rich stroma, MT1-MMP/MMP-2 seems to act as a potent type I collagen degradation system, and MT1-MMP is highly sensitive to TIMP-2 (Sabeh et al. 2004). In addition to their MMP-inhibitory activity, TIMPs are now widely considered to exert pluripotential effects on cellular behavior such as cell growth, survival, migration, and differentiation, independently of their MMP neutralizing functions (Baker et al. 2002). TIMP-2 can either inhibit (Murphy et al. 1993) or promote (Hayakawa et al. 1994) cell growth. Recently, TIMP-2 has been shown to be the ligand of integrin α3β1, and ligand binding directly inhibits the proliferation of endothelial cells (Seo et al. 2003). Of the four known TIMPs, TIMP-2 has been thought to be soluble and not to bind to ECM, in contrast to TIMP-3 (Yu et al. 2000). However, our previous data have indicated that TIMP-2 also binds to ECM in a peculiar distribution pattern during tooth development in mouse from embryonic day (E)13 to postnatal day (P)3 (Yoshiba et al. 2003, 2006).

Teeth are formed from ectoderm-derived oral epithelial and neural-crest-derived ectomesenchymal cells. The dental epithelium invaginates into the mesenchyme and forms the tooth bud (E13), cap (E14), and the bell (E16), at which time the shape of the tooth crown is established. The epithelium then gives rise to enamel. The condensed mesenchyme forms the dental papilla and dental follicle, which give rise to odontoblasts, cementoblasts, periodontal ligaments, and alveolar bone. Continuously erupting incisors of rodents contain a stem cell compartment (the apical loop) at the apical end, which consists of stem cells for all types of epithelia of incisors. From the bud to early bell stages of molar tooth development, TIMP-2 has been shown to be associated with the ECM in the jaw mesenchyme on the lingual side of the molar germ and along the lingual side of the dental basement membrane (Yoshiba et al. 2003). At P3, TIMP-2 accumulates on both sides of the molar germ (Yoshiba et al. 2003). During incisor development (E14-P3), TIMP-2 is restricted to the basement membrane of the apical loop. In contrast to the restricted localization of TIMP-2, *Timp-2* mRNA is broadly expressed (Yoshiba et al. 2003, 2006).

Periostin is an ECM protein that was originally isolated from an osteoblastic cell line and was first known as osteoblast-specific factor 2 (Osf-2; Takeshita et al. 1993). Thereafter, Osf-2 was renamed to periostin, because of its preferential expression in the periosteum and periodontal ligaments; it has been reported to support osteoblastic cell attachment and spreading (Horiuchi et al. 1999). Periostin is highly homologous to βig-h3, previously known as transforming growth factor-β (TGF-β)-inducible protein. Both periostin and βig-h3 contain fasciclin (Fas-1) domains (Takeshita et al. 1993; Skonier et al. 1994). The Fas-1 domains of βig-h3 have been shown to interact with integrin α3β1 of epithelial cells (Kim et al. 2000) and with integrin αvβ5 of mesenchymal cells (Kim et al. 2002). Thus, Fas-1 domain-containing proteins are suggested to perform their biological functions by interacting with integrins (Kim et al. 2002). On the other hand, periostin has also been shown to mediate cell adhesion by binding to integrins αvβ3 and αvβ5 (Gillan et al. 2002). Furthermore, periostin is suggested to bind to integrin α3β1, because of the existence of suitable binding sites in Fas-1 domains (Kudo et al. 2004). Recently, two laboratories have generated *periostin* null mice (Rios et al. 2005; Kii et al. 2006). These null mice have abnormal postnatal incisors, suggesting the critical requirement of periostin for the integrity of periodontal ligaments in response to mechanical stresses (Rios et al. 2005) and its function in the remodeling of the collagen matrix in the shear zone (Kii et al. 2006). In addition to their localization in

periodontal ligaments, periostin mRNA and protein have been shown to be present at higher levels on the lingual side of the mouse molar tooth germ compared with the buccal side (Kruzynska-Frejtag et al. 2004), and the surface of the apical loop in postnatal mouse incisors shows weak positive reactivity for periostin (Suzuki et al. 2004). Although the localization of periostin has not been fully analyzed during molar and incisor tooth morphogenesis, the reported localization of periostin is intriguingly similar to that of TIMP-2 mentioned above. *Timp-2* mRNA is expressed in periodontal ligaments and in tendons. However, whether TIMP-2 can associate with ECM in these tissues remains unknown.

In order to test the hypothesis that TIMP-2 can associate with ECM of specific areas and co-distribute with periostin, we have analyzed the tissue distribution patterns of TIMP-2 and periostin in mouse mandible development by using immunohistochemistry. Furthermore, the dissected mandible has been cultured in the presence of anti-TIMP-2 antibody, and the localization of periostin has been evaluated.

Materials and methods

Preparation of tissues

Heads of mouse embryos at E13–E16 and P2 were embedded in Tissue-Tek O.C.T. Compound (SAKURA), frozen in liquid nitrogen, and cut as 8-μm-thick frontal or sagittal sections. Lingual gingival tissues of adult mice were isolated, and cryosections were prepared as described above. Mandibles at P35 and P12 weeks were also frozen, and cryosections were prepared.

Indirect immunofluorescence

Immunostaining with antibodies raised against periostin (1:50 dilution; BioVender, Heidelberg, Germany), TIMP-1 (1:100 dilution; R&D Systems, Minneapolis, Minn.), TIMP-2 (1:100 dilution; Chemicon, Temecula, Calif.), TIMP-3 (1:100 dilution; Chemicon), laminin (1:400; Sigma, St. Louis, Mo.), and integrin α3 (1:400 dilution; BD, N.J.) was performed on cryosections as previously described (Yoshiba et al. 2003). Briefly, cryosections were fixed in cooled acetone, washed in phosphate-buffered saline (PBS), and incubated with the primary antibodies followed by Cy3-conjugated secondary antibodies (1:500 dilution; Jackson Immunoresearch, West Grove, Pa.).

In situ hybridization

TIMP-2 cDNA (Leco et al. 1992) was kindly provided by Dr. Robert Nuttall (University of East Anglia, Norfolk, UK). The [^{35}S]CTP-labeled sense and antisense riboprobes were prepared by in vitro transcription. In situ hybridization on cryosections was performed as described previously (Yoshiba et al. 2003).

Organ culture experiments

Gingival tissue with the associated molar was dissected from the mandible at P2 and cultured for 4 days in serum-free DMEM supplemented with penicillin/streptomycin. For antibody inoculation, anti-TIMP-2 antibody was added to the culture medium at a concentration of 50 μg/ml. Antibodies against TIMP-1 and TIMP-3 were used as controls at the same concentration. The cultured tissue was embedded in Tissue-Tek, and cryosections were prepared. Immunofluorescence was performed as described above.

Results

Localization of TIMP-2 and periostin in mandible at E14

TIMP-2 was localized in specific areas of sagittal sections of mandibles at E14 (Fig. 1a). Pronounced immunoreaction of TIMP-2 was observed in the jaw mesenchyme at the anterior part of the molar (Fig. 1a, b) and in the tendon of Ramus of the mandible (Fig. 1a, arrows). Intriguingly, in sagittal serial sections, periostin showed the same distribution pattern as TIMP-2. The jaw mesenchyme at the anterior part of the molar was abundant in periostin (Fig. 1c). In contrast, the posterior part of the molar was devoid of both proteins (Fig. 1b, c, asterisks). In serial frontal sections, TIMP-2 and periostin were found to be present along the dental basement membrane on the lingual side of the molar and on the adjacent jaw mesenchyme (Fig. 1d, e). In contrast, the jaw mesenchyme on the buccal side was devoid of both proteins (Fig. 1d, e, asterisks). TIMP-2 appeared to associate with the ECM (Fig. 1b, d, f). On the other hand, periostin was observed on the cell surface (Fig. 1g). TIMP-2 has been reported to bind to integrin α3 (Seo et al. 2003), and periostin has been suggested to be a ligand of integrin (Kudo et al. 2004). Hence, the localization of integrin α3 was analyzed. Integrin α3 was readily recognized on the lingual side of the dental epithelium at E13 (Fig. 1h) and E14 (Fig. 1i), and its reactivity decreased at E16 (data not shown). The localization pattern of integrin α3 was in agreement with those of TIMP-2 and periostin on the basement membrane.

Localization of TIMP-2 and periostin in mandible at E16

TIMP-2 and periostin showed the same distribution patterns at E16. Both proteins were localized in tendons (Fig. 2a, c, d), but their staining patterns were different (Fig. 2c, d). On

the molar germ at the bell stage, TIMP-2 (Fig. 2e) and periostin (Fig. 2f) disappeared from the basement membrane, except on the lingual side of the dental lamina. In the jaw mesenchyme, both proteins were detected on the lingual side, the buccal side being devoid of TIMP-2 and periostin (Fig. 2e, f, asterisks). Detailed analysis revealed that TIMP-2 was apparently associated with the ECM in the jaw mesenchyme (Fig. 2g), whereas periostin demonstrated a punctate pattern combined with fine fibrils (Fig. 2h).

Localization of TIMP-2 and periostin in gingival tissues at P2 and in adult mice

TIMP-2 (Fig. 3a) and periostin (Fig. 3b) accumulated in the jaw mesenchyme on both sides of the molar germ at P2 in an area that corresponded to future gingival tissues. They were present on the ECM and on fibers connecting to the alveolar bone (Fig. 3d, e, arrows). In adult mice, TIMP-2 remained accumulated in gingival tissues (Fig. 3f). Periostin was also abundantly detected in gingival tissues (data not shown). TIMP-3 has been suggested to be an ECM-binding protein. Hence, we analyzed the localization of TIMP-3 and TIMP-1 in adult gingival tissues. In contrast to TIMP-2, neither TIMP-1 (Fig. 3g) nor TIMP-3 (Fig. 3h) was restricted to gingival tissues. To support the immunohistochemical results with respect to TIMP-2, the expression of *Timp-2* mRNA was analyzed at P2. *Timp-2* was strongly expressed in the periodontal tissues, including the periodontal ligaments (Fig. 3j, arrows) and gingival tissues (Fig. 3k).

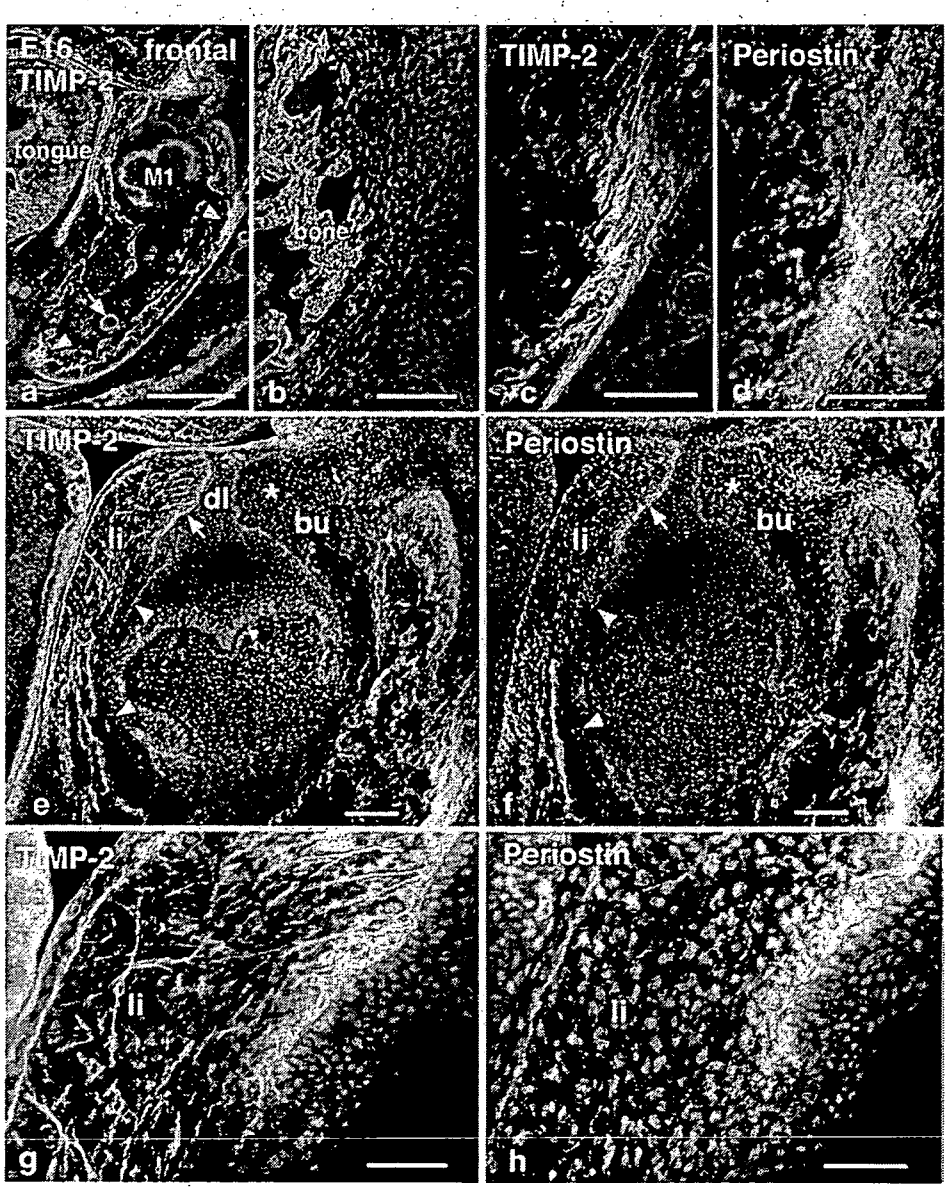

Fig. 2 Immunohistochemical detection of TIMP-2 and periostin in the mandible at E16. **a** Low-power image of a frontal section of the mandible stained with TIMP-2 (*arrowheads* expression of TIMP-2 in the tendon, *arrow* expression of TIMP-2 on basement membrane of apical loop of incisor). **b–d** A higher power image of the area indicated by the *arrowhead* (*right*) in **a** is presented in **c**, and its phase-contrast image is shown in **b**. **d** Serial section to that in **c** immunostained for periostin. TIMP-2 (**c**) and periostin (**d**) distribution patterns are similar. **e, f** Serial frontal sections showing TIMP-2 and periostin expression, respectively. Both proteins disappear from the basement membrane on the lingual side (*li*, *arrowheads*), although they are detectable along the dental lamina (*dl*) on the lingual side (*arrow*). In the jaw mesenchyme, both proteins are localized on the lingual side; in contrast, the buccal side (*bu*) is devoid of TIMP-2 and periostin (*asterisks*). **g, h** Higher power views of the lingual jaw mesenchyme of **e, f**, respectively. *Bars* 500 μm (**a**), 100 μm (**b–f**), 50 μm (**g, h**)

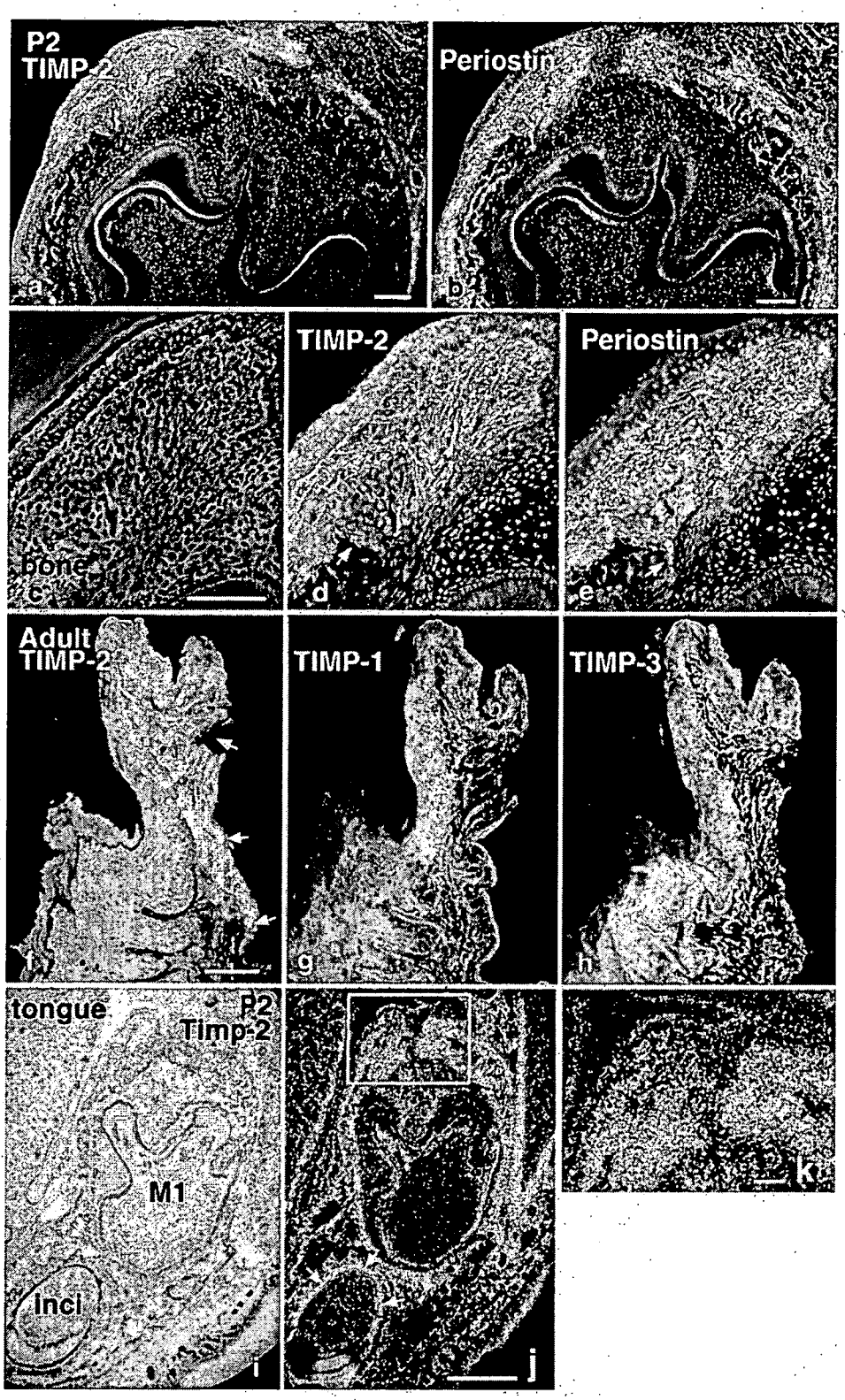
P2
TIMP-2
a
Periostin
b
Bone
c
TIMP-2
d
Periostin
e
Adult
TIMP-2
f
TIMP-1
g
TIMP-3
h
tongue
P2
Timp-2
M1
Incl
i
j
k

◀ **Fig. 3** Immunohistochemical detection of TIMP-2 and periostin in gingival tissues at postnatal day 2 (P2) and in adult mouse, and in situ hybridization analysis of TIMP-2 at P2. **a**, **b** Serial frontal sections stained with TIMP-2 and periostin, respectively. The jaw mesenchyme is strongly stained with TIMP-2 and periostin on both sides of the molar germ at P2. **c–e** High-power images of **a**, **b** are presented in **d**, **e**, respectively; **c** is the phase-contrast image of **d**. Although both proteins are visible on the ECM, their staining patterns are different. Fibers connecting to alveolar bone are also stained with both proteins (**d**, **e**, *arrows*). **f–h** TIMP-2 is strongly detected in gingiva of adult mouse (**f**, *arrows*). In contrast, neither TIMP-1 (**g**) nor TIMP-3 (**h**) is restricted to gingival tissues. **i–k** In situ hybridization analysis of TIMP-2 at P2. **i** Bright-field image of **j** (*M1* first molar, *inci* incisor). **k** Higher power view of *boxed area* in **j**. *Timp-2* transcripts are detected in the periodontal ligament (**j**, *arrows*) and gingival tissue (**k**). *Bars* 500 μm (**j**), 100 μm (**a–c**, **f**, **k**)

Localization of TIMP-2 in periodontal ligament at P35 and 12 weeks

The periodontal ligament is a soft connective tissue that serves to anchor the tooth to the alveolar bone and functions as a cushion between two mineralized tissues. Expression of periostin is temporospatially regulated in the periodontal ligament, which is broadly stained with periostin at P21 in mouse (Suzuki et al. 2004).

Hence, the localization of TIMP-2 was analyzed in periodontal ligaments. In frontal sections of mandibles at P35, strong TIMP-2 immunoreactivity was partially seen in periodontal ligaments (Fig. 4a, arrows). TIMP-2 was strongly detected on the alveolar bone or cementum side

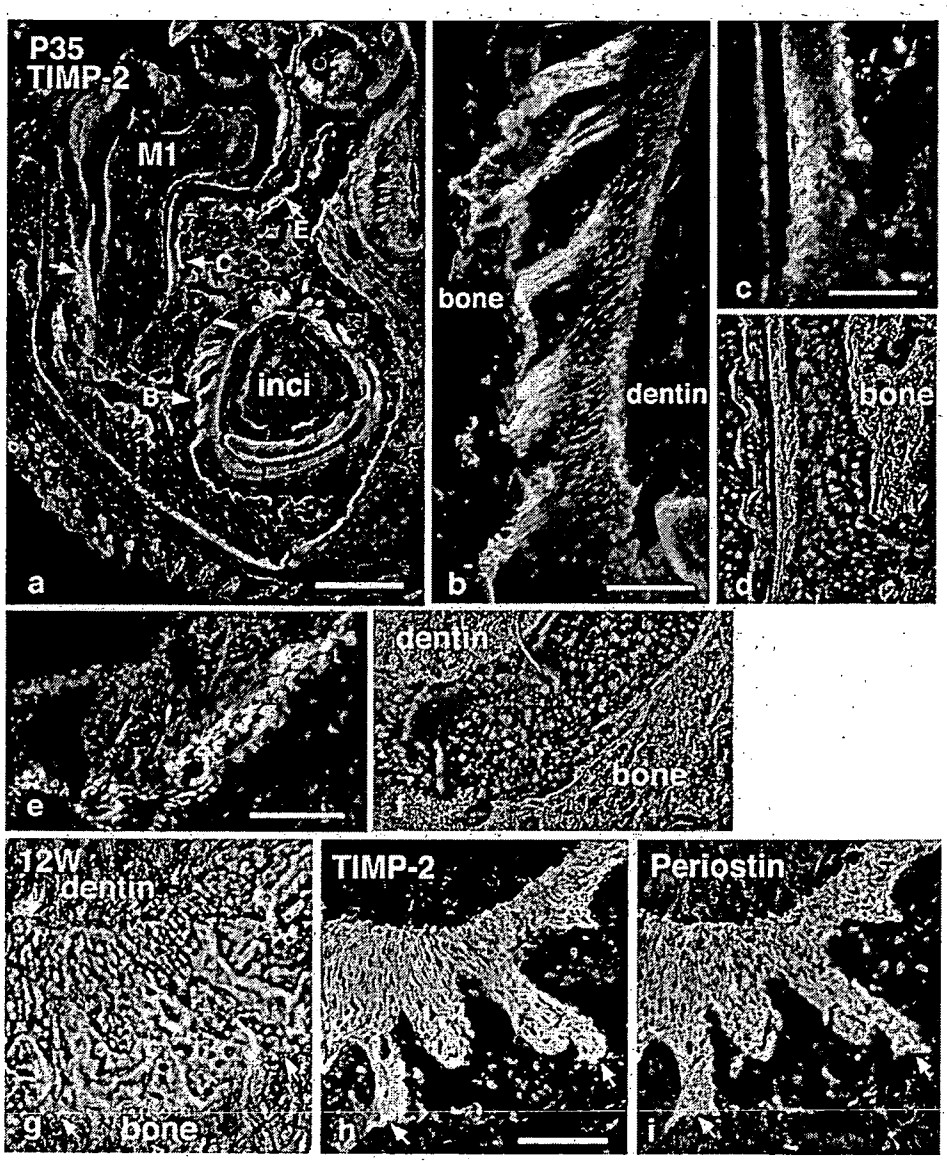

Fig. 4 Immunohistochemical detection of TIMP-2 in the periodontal ligament at P35 and 12 weeks of age. **a** Low-power image of a frontal section of mandible stained with TIMP-2 (*arrows* expression of TIMP-2 in the periodontal ligament of the molar and incisor, *M1* molar, *inci* incisor). **b–f** High-power images of the areas indicated as *B*, *C*, *E* in **a** are shown in **b**, **c**, **e**, respectively. **d**, **f** Phase-contrast images of **c**, **e**, respectively. A part of the periodontal ligament is strongly stained with TIMP-2. **g–i** A phase-contrast image of **h** is presented in **g**. TIMP-2 (**h**) and periostin (**i**) are broadly detected in the periodontal ligament at 12 weeks of age (*arrows* junctions between the ligament and alveolar bone). *Bars* 500 μm (**a**), 100 μm (**b–h**)

of the ligament (Fig. 4b, c, e). TIMP-2 was broadly observed in the periodontal ligament at 12 weeks (Fig. 4h) and thus had a distribution similar to that of periostin (Fig. 4i).

Localization of TIMP-2 and periostin in mandibular joint at P2

In order to confirm that TIMP-2 associated with the ECM of tendons, the mandibular joint at P2 was analyzed. TIMP-2 (Fig. 5c, e) and periostin (Fig. 5g, h) were similarly distributed in this tissue. TIMP-2 was clearly immunostained in the ECM of the tendon (Fig. 5e, arrows). In contrast, the ECM of the tendon was devoid of TIMP-3 (Fig. 5f, arrows). To support the immunohistochemical results of TIMP-2 expression, the expression of *Timp-2* mRNA was analyzed. *Timp-2* transcripts were detectable in the tendon (Fig. 5a, b, arrows).

Localization of TIMP-2 and periostin during incisor development

The temporospatial distribution of TIMP-2 and periostin was similar and specific during molar tooth development. The distribution patterns of TIMP-2 and periostin were further examined during incisor tooth development. The basement membrane of the incisor was initially devoid of both TIMP-2 and periostin at E13 (bud stage, data not shown). At the early bell stage of E14, TIMP-2 was weakly expressed on the basement membrane of the apical loop, whereas periostin was negligibly detected at this position and at this stage (data not shown). At the bell stages of E16 and P2 (Fig. 6c), periostin was detectable on the basement membrane of the apical loop, in addition to TIMP-2 (Fig. 6b). Both proteins could also be recognized in the dental follicle (Fig. 6b, c). Detailed inspection of the basement membrane and the dental follicle revealed differences in immunostaining patterns of periostin and TIMP-2 (Fig. 6d, e).

Localization of TIMP-2 and periostin in skin at P2

TIMP-2 and periostin asymmetrically colocalized on the dental basement membrane during tooth development. The basement membrane of skin (also exposed to mechanical force) was additionally analyzed. TIMP-2 and periostin colocalized along the basement membrane of the epidermis and the upper part of the outer root sheath of hair follicles (Fig. 7b, c, double arrows). Unexpectedly, periostin was solely detected on the lower portion of the inner root sheath (Fig. 7c, arrows). The upper part of the inner root sheath was devoid of periostin (Fig. 7c, arrowheads).

Loss of periostin immunoreactivity in gingiva cultured with anti-TIMP-2 antibody

TIMP-2 and periostin were significantly co-distributed in vivo. Therefore, we investigated their functional relationships in vitro. As TIMP-2 and periostin were abundantly

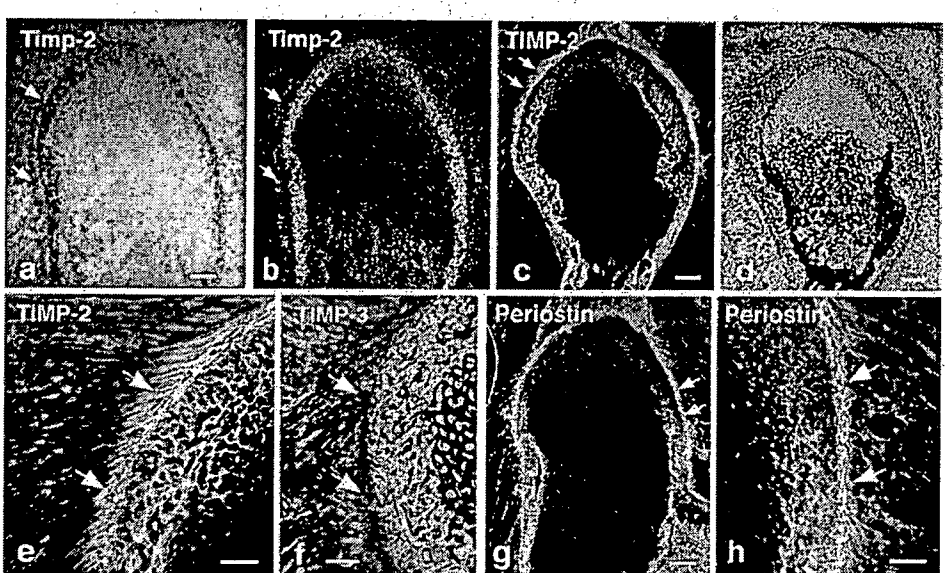

Fig. 5 Immunohistochemical detection of TIMP-2 and periostin, and in situ hybridization analysis of TIMP-2 in the mandibular joint at P2. **a, b** In situ hybridization analysis of TIMP-2. **a** Bright-field image of **b**. *Timp-2* transcripts are detected in tendons (*arrows*). **c–e** TIMP-2 protein localization in the mandibular joint. **d** Phase-contrast image of **c**. **e** Higher power view of the area indicated by *arrows* in **c**. TIMP-2 protein is associated with the ECM of the tendon (**e**, *arrows*). **f** TIMP-3 is not detected in the ECM of the tendon (*arrows*). **g** Low-power image of immunostaining for periostin. **h** Higher power view of the area indicated by *arrows* in **g**. Periostin is localized on the tendon (**h**, *arrows*). *Bars* 100 μm (**a**, **c**, **d**, **g**), 50 μm (**e**, **f**, **h**)

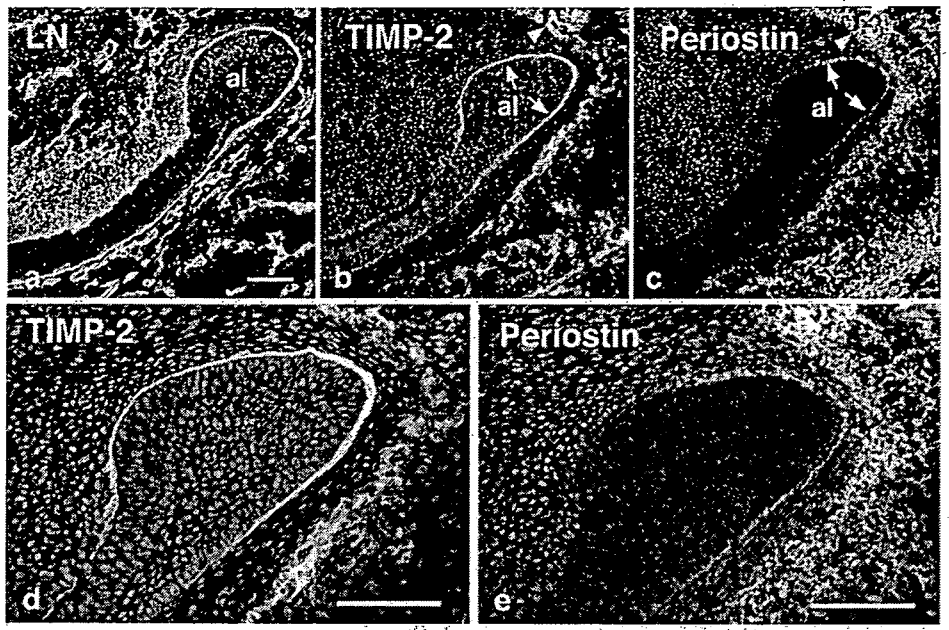

Fig. 6 Immunohistochemical detection of TIMP-2 and periostin in the incisor at P2. **a** Labeling of the basement membrane of the incisor for laminin (*LN*). **b, c** TIMP-2 (**b**) and periostin (**c**) are restricted to the basement membrane of the apical loop (*al, arrows*) and to the dental follicle (*arrowhead*). **d, e** High-power images of **b, c**, respectively. Immunostaining patterns are different between TIMP-2 and periostin. *Bars* 100 μm

present on the ECM of gingival tissues at P2 (Fig. 3a, b), gingiva at P2 was dissected with the molar germ,and cultured for 4 days with or without anti-TIMP-2 antibody. In the absence of anti-TIMP-2 antibody, the ECM of the cultured gingiva was strongly positive for TIMP-2 (Fig. 8a) and periostin (Fig. 8b). Neutralization of TIMP-2 with anti-TIMP-2 antibody resulted in a loss of staining of periostin in the gingiva (Fig. 8c, d). The specificity of the anti-TIMP-2 antibody effect on periostin was demonstrated by culturing gingiva with anti-TIMP-1 or anti-TIMP-3 antibody. Periostin could still be localized in anti-TIMP-1-treated (Fig. 8e, f) and anti-TIMP-3-treated (Fig. 8g, h) tissues.

Discussion

In this study, we have demonstrated that TIMP-2 protein coexists with the ECM of specific tissues, e.g., gingiva, periodontal ligaments, and tendons, which are all constantly exposed to mechanical forces. Furthermore, TIMP-2 is asymmetrically localized on the dental basement membrane. The tissue distribution of TIMP-2 is temporospatially regulated and corresponds remarkably to that of periostin.

Both TIMP-2 and periostin are secreted proteins and seem to be associated with the ECM. However, their abilities to bind to ECM components seem to be inconsis-

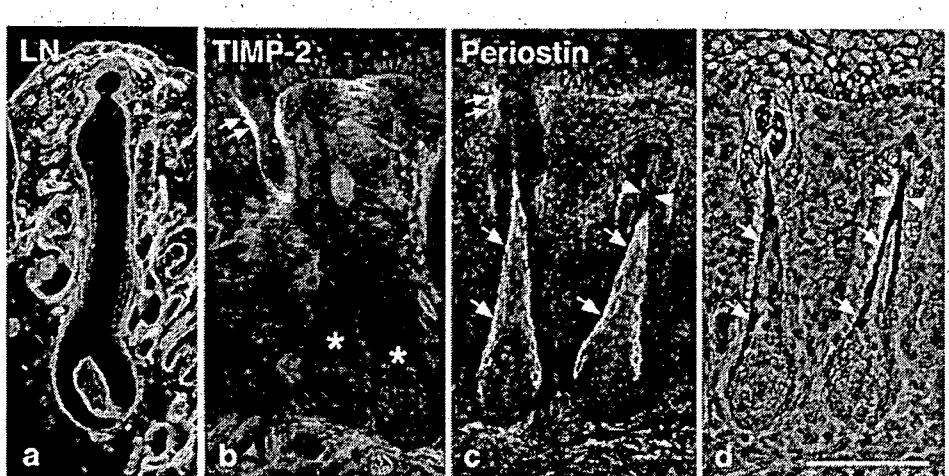

Fig. 7 Immunohistochemical detection of TIMP-2 and periostin in skin at P2. **a** Labeling of the basement membrane of the hair follicle for laminin (*LN*). **b** TIMP-2 is present on the basement membrane of the epidermis and the upper part of the outer root sheath of the hair follicle (*double arrow*). The lower part of the hair follicle is devoid of TIMP-2 (*asterisks*). **c, d** A phase-contrast image of **c** is shown in **d**. Periostin is also present on the basement membrane of the epidermis and the upper part of the outer root sheath of the hair follicle (*double arrow*). Notably, periostin is solely detected on the lower portion of the inner root sheath (*arrows* in **c**). The upper part of the inner root sheath is devoid of periostin (**c**, *arrowheads*). *Bar* 100 μm

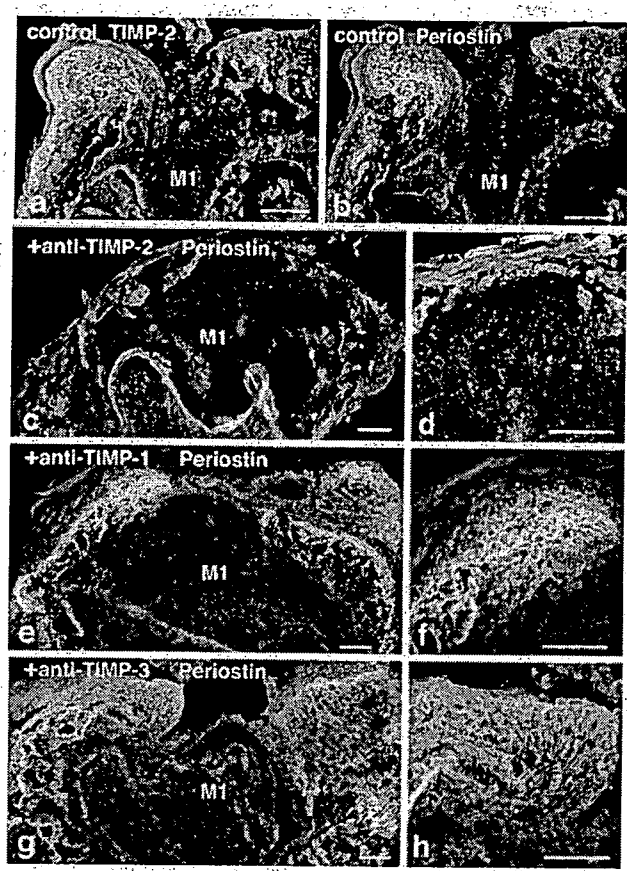

Fig. 8 Loss of staining of periostin in gingiva cultured with anti-TIMP-2 antibody (*M1* molar). **a**, **b** TIMP-2 (**a**) and periostin (**b**) are strongly detectable in the ECM of gingival tissues cultured in control medium. **c**, **d** Higher power view of the gingival tissue in **c** is presented in **d**. Periostin is not detectable in gingival tissue cultured in medium conditioned with anti-TIMP-2 antibody. **e**–**h** Higher power views of gingival tissues in **e**, **g** are presented in **f**, **h**, respectively. Neutralization of TIMP-1 (**e**, **f**) or TIMP-3 (**g**, **h**) does not alter the localization of periostin in gingival tissues. *Bars* 100 μm

tent. The typical ECM proteins in tendinous connective tissues, periodontal ligaments, and gingival tissues are types I and III collagens, tenascin-C, and fibronectin. A binding assay has shown that periostin binds to ECM proteins such as tenascin-C, fibronectin, collagen V, and periostin itself, but not to collagens I and III, and Fas-1 domains in periostin are responsible for these bindings (Takayama et al. 2006). On the other hand, an immunoelectron-microscopical analysis has suggested that periostin binds to type I collagen in periodontal ligaments in vivo (Kii et al. 2006). In contrast to periostin, no reports are available on binding assays of TIMP-2 to ECM components. Among the TIMP family, TIMP-3 is well known to have a specific ECM-binding domain and associates directly with heparan sulfate proteoglycans (Yu et al. 2000). Interestingly, the tissue distributions of TIMP-2 and TIMP-3 are significantly different in our study, emphasizing the role of TIMP-2 in tissues affected by mechanical strain. The binding mechanism of TIMP-2 to ECM components remains to be established. In our in vitro study, TIMP-2 is abundantly expressed in cultured P2 jaw mesenchyme (Fig. 8a); however, TIMP-2 is not detectable in cultured E14 jaw mesenchyme (data not shown). Furthermore, TIMP-2 expression in the ECM of periodontal ligaments is delayed compared with that of periostin. Thus, the maturation of collagen fibrils might be related to the binding of TIMP-2 to the ECM. The expression of TIMP-2 and periostin in the jaw mesenchyme is temporospatially regulated; the stained mesenchyme extends from the lingual to buccal areas and in an anterior to posterior direction and gives rise to gingival tissues. Developmental mechanisms of gingival tissues remain unknown, although the distribution of TIMP-2 and periostin might be related to gingival development. Although TIMP-2 and periostin are similarly distributed, their staining patterns are significantly different. TIMP-2 appears to be associated with the ECM from an early stage of development, whereas periostin shows a punctate pattern combined with fibrils. Recently, the association of periostin with Notch 1 has been reported (Tanabe et al. 2004); this might be related to its punctate expression.

ECM composition appears to be regulated by mechanical stresses placed on cells in connective tissues (Banes et al. 2001). Mechanical stress affects the expression of MMPs and TIMPs in various cell types (Bolcato-Bellemin et al. 2000; Tsuji et al. 2004; He et al. 2004). Stretch applied to periodontal ligaments and gingival fibroblasts induces the expression of *Mmp-1*, *Mmp-2*, *Timp-1*, and *Timp-2* mRNAs, whereas that of *Mt1-mmp* is not varied (Bolcato-Bellemin et al. 2000; He et al. 2004). Intermittent tensile stress to periodontal ligament cells increases the expression of *Timp-1* and *Timp-2* mRNAs, but barely affects that of *Mmp-1* and *Mmp-2* mRNA, suggesting that appropriate stress acts as an inhibitor of the degradation of ECM in the periodontal ligament (Tsuji et al. 2004). In rat tendon, MMP-2 and MT1-MMP, whose activities are strongly controlled by TIMP-2, have been shown to participate not only in collagen degradation, but also in collagen remodeling (Oshiro et al. 2003). In addition to its MMP inhibition activity, TIMP-2 can provoke a significant increase in fibroblast collagen synthesis (Lovelock et al. 2005). On the other hand, mechanical stress also alters *periostin* mRNA expression. Periostin expression increases under pressure from orthodontic tooth movement (Wilde et al. 2003) and decreases during occlusal hypofunction in the mouse periodontal ligament (Afanador et al. 2005). Periostin null mice placed on a soft diet that alleviates mechanical strain on the periodontal ligament show partial rescue of periodontal disease-like phenotypes (Rios et al. 2005). Furthermore, periostin has been suggested to digest collagen fibers in the shear zone of the mouse incisor periodontal ligament (Kii et al. 2006). Thus, TIMP-2 and periostin appear to play key roles in maintaining the

homeostasis of tissues receiving mechanical strain. MMPs can degrade all ECM components, although which MMPs can cleave periostin remain unknown. In our in vitro study, the localization patterns of periostin drastically alter in gingival tissues cultured in anti-TIMP-2 antibody-conditioned medium (Fig. 8c, d). In contrast, the addition of anti-TIMP-1 or anti-TIMP-3 antibodies does not affect periostin distribution (Fig. 8e–h). TIMP-2 may protect the degradation of periostin from MMP activities.

In addition to their similar tissue distributions, TIMP-2 and periostin have similar properties with regard to cellular behavior, and multiple reports have independently shown their close correlations with metastatic growth in cancer. Both proteins affect cytodifferentiation. TIMP-2 induces the differentiation of cardiac fibroblasts (Lovelock et al. 2005) and skeletal muscles (Lluri and Jaworski 2005), whereas periostin is correlated with smooth muscle cell differentiation (Lindner et al. 2005). TIMPs (Edwards et al. 1987; Overall et al. 1991) and periostin (Horiuchi et al. 1999) can be induced by TGF-β1, which is known to stimulate ECM protein synthesis via Smad proteins (Zhang et al. 2000; Arai et al. 2002; Lindahl et al. 2002). An association between TGF-β1 and mechanical loading has also been demonstrated in a number of cell and tissue types. Stretch-force-induced TGF-β1 expression has been shown in tendons (Skutek et al. 2001), cardiac fibroblasts (Ruwhof et al. 2000; Lindahl et al. 2002), and osteoblast-like cells (Klein-Nulend et al. 1995). Fibroblasts overexpressing TGF-β1 show increased TIMP-2 expression more significantly than other TIMPs, suggesting effects of TGF-β1 on the MMP/TIMP system (Seeland et al. 2002). TGF-β1 and its inducers, TIMP-2 and periostin, may coordinately function as ECM modulators in tissues that experience mechanical strain.

Integrin α3β1 appears to be the common integrin to which TIMP-2 (Seo et al. 2003) and periostin (Kudo et al. 2004) can bind. This has been confirmed in the early stages of molar tooth morphogenesis, at which time TIMP-2, periostin, and integrin α3 are all clearly detectable along the outer dental epithelium on the lingual side. In contrast, the buccal side is devoid of these proteins (Fig. 1d, e, h, i). On the contrary, laminin-5 (α3β3γ2), which is associated with several epithelial tissues, has been detected at a much higher intensity on the buccal side rather than the lingual side of the basement membrane at E14 (Yoshiba et al. 1998a). During normal developmental tissue growth, the basement membrane is subjected to increased mechanical strain. Local stress changes are suggested to control basement membrane remodeling by Rho, a small GTPase, and cytoskeletal tension (Moore et al. 2005; Ingber 2006). TIMP-2 promotes the association of Rap 1, the closest homolog of the small GTPase Ras, with actin (Chang et al. 2006). Rho and Ras signaling, which regulates the organization of the actin cytoskeleton, are involved in submandibular gland development through integrin α3β1 (Menko et al. 2001). Laminin-5 is also involved in epithelial morphogenesis (Baker et al. 1996; Stahl et al. 1997). The differential localization of these proteins on the dental basement membrane may indicate that the morphogenesis of molar teeth is asymmetrically regulated. In incisors, TIMP-2 and periostin have been specifically detected on the basement membrane of the apical loop (Fig. 6) from the early bell stage of development, at which time laminin-5 is also strongly detectable (Yoshiba et al. 1998b). Further studies should elucidate any interactive functions among these molecules on the basement membrane.

A novel constructor of tissue junctions, viz., collagen XXII, has recently been reported (Koch et al. 2004). Collagen XXII is strictly restricted to tissue junctions in muscles, tendons, heart, and articular cartilage. Notably, the immunostaining pattern of collagen XXII in hair follicles is surprisingly similar to that of periostin demonstrated in our study (Fig. 7c) in which collagen XXII and periostin have been found in the lower part of hair follicles with a sheath-like staining pattern. Periostin was originally identified as a homophilic adhesion molecule (Takeshita et al. 1993). Thus, the localization of both proteins suggests the presence of a junctional structure between multiple epithelial layers in hair follicles (Langbein et al. 2002).

In conclusion, TIMP-2 protein associates with the ECM of tissues that are exposed to mechanical forces, from early stages of development. Furthermore, the tissue distribution of TIMP-2 is strikingly similar to that of periostin. Both proteins also colocalize on the dental basement membrane during tooth morphogenesis, and their distribution patterns are asymmetrically and spatiotemporally regulated. Additional studies may determine their potential roles and functional relationships in ECM remodeling.

Acknowledgements The authors thank Prof. Dylan Edwards and Dr. Robert Nuttall (University of East Anglia, Norfolk, UK) for their generous gift of the cDNA for TIMP-2.

References

Afanador E, Yokozeki M, Oba Y, Kitase Y, Takahashi T, Kudo A, Moriyama K (2005) Messenger RNA expression of periostin and Twist transiently decrease by occlusal hypofunction in mouse periodontal ligament. Arch Oral Biol 50:1023–1031

Arai K, Kasashima Y, Kobayashi A, Kuwano A, Yoshihara T (2002) TGF-beta alters collagen XII and XIV mRNA levels in cultured equine tenocytes. Matrix Biol 21:243–250

Baker SE, Hopkinson SB, Fitchmun M, Andreason GL, Frasier F, Plopper G, Quaranta V, Jones JC (1996) Laminin-5 and hemidesmosomes: role of the alpha 3 chain subunit in hemidesmosome stability and assembly. J Cell Sci 109:2509–2520

Baker AH, Edwards DR, Murphy G (2002) Metalloproteinase inhibitors: biological actions and therapeutic opportunities. J Cell Sci 115:3719–3727

Banes AJ, Lee G, Graff R, Otey C, Archambault J, Tsukazi M, Elfervig M, Qi J (2001) Mechanical forces and signaling in connective tissue cells: cellular mechanisms of detection, transduction, and responses to mechanical deformation. Curr Opin Orthop 12:389–396

Bolcato-Bellemin AL, Elkaim R, Abehsera A, Fausser JL, Haikel Y, Tenenbaum H (2000) Expression of mRNAs encoding for alpha and beta integrin subunits, MMPs, and TIMPs in stretched human periodontal ligament and gingival fibroblasts. J Dent Res 79:1712–1716

Chang H, Lee J, Poo H, Noda M, Diaz T, Wei B, Stetler-Stevenson WG, Oh J (2006) TIMP-2 promotes cell spreading and adhesion via upregulation of Rap1 signaling. Biochem Biophys Res Commun 345:1201–1206

Edwards DR, Murphy G, Reynolds JJ, Whitham SE, Docherty AJ, Angel P, Heath JK (1987) Transforming growth factor beta modulates the expression of collagenase and metalloproteinase inhibitor. EMBO J 6:1899–1904

Gillan L, Matei D, Fishman DA, Gerbin CS, Karlan BY, Chang DD (2002) Periostin secreted by epithelial ovarian carcinoma is a ligand for alpha(V)beta(3) and alpha(V)beta(5) integrins and promotes cell motility. Cancer Res 62:5358–5364

Hayakawa T, Yamashita K, Ohuchi E, Shinagawa A (1994) Cell growth-promoting activity of tissue inhibitor of metalloproteinases-2 (TIMP-2). J Cell Sci 107:2373–2379

He Y, Macarak EJ, Korostoff JM, Howard PS (2004) Compression and tension: differential effects on matrix accumulation by periodontal ligament fibroblasts in vitro. Connect Tissue Res 45:28–39

Horiuchi K, Amizuka N, Takeshita S, Takamatsu H, Katsuura M, Ozawa H, Toyama Y, Bonewald LF, Kudo A (1999) Identification and characterization of a novel protein, periostin, with restricted expression to periosteum and periodontal ligament and increased expression by transforming growth factor beta. J Bone Miner Res 14:1239–1249

Ingber DE (2006) Mechanical control of tissue morphogenesis during embryological development. Int J Dev Biol 50:255–266

Kii I, Amizuka N, Minqi L, Kitajima S, Saga Y, Kudo A (2006) Periostin is an extracellular matrix protein required for eruption of incisors in mice. Biochem Biophys Res Commun 342:766–772

Kim JE, Kim SJ, Lee BH, Park RW, Kim KS, Kim IS (2000) Identification of motifs for cell adhesion within the repeated domains of transforming growth factor-beta-induced gene, beta ig-h3. J Biol Chem 275:30907–30915

Kim JE, Jeong HW, Nam JO, Lee BH, Choi JY, Park RW, Park JY, Kim IS (2002) Identification of motifs in the fasciclin domains of the transforming growth factor-beta-induced matrix protein beta ig-h3 that interact with the alphavbeta5 integrin. J Biol Chem 277:46159–46165

Klein-Nulend J, Roelofsen J, Sterck JG, Semeins CM, Burger EH (1995) Mechanical loading stimulates the release of transforming growth factor-beta activity by cultured mouse calvariae and periosteal cells. J Cell Physiol 163:115–119

Knauper V, Will H, Lopez-Otin C, Smith B, Atkinson SJ, Stanton H, Hembry RM, Murphy G (1996a) Cellular mechanisms for human procollagenase-3 (MMP-13) activation. Evidence that MT1-MMP (MMP-14) and gelatinase a (MMP-2) are able to generate active enzyme. J Biol Chem 271:17124–17131

Knauper V, Lopez-Otin C, Smith B, Knight G, Murphy G (1996b) Biochemical characterization of human collagenase-3. J Biol Chem 271:1544–1550

Koch M, Schulze J, Hansen U, Ashwodt T, Keene DR, Brunken WJ, Burgeson RE, Bruckner P, Bruckner-Tuderman L (2004) A novel marker of tissue junctions, collagen XXII. J Biol Chem 279:22514–22521

Kruzynska-Frejtag A, Wang J, Maeda M, Rogers R, Krug E, Hoffman S, Markwald RR, Conway SJ (2004) Periostin is expressed within the developing teeth at the sites of epithelial-mesenchymal interaction. Dev Dyn 229:857–868

Kudo H, Amizuka N, Araki K, Inohaya K, Kudo A (2004) Zebrafish periostin is required for the adhesion of muscle fiber bundles to the myoseptum and for the differentiation of muscle fibers. Dev Biol 267:473–487

Langbein L, Rogers MA, Praetzel S, Aoki N, Winter H, Schweizer J (2002) A novel epithelial keratin, hK6irs1, is expressed differentially in all layers of the inner root sheath, including specialized Huxley cells (Flugelzellen) of the human hair follicle. J Invest Dermatol 118:789–799

Leco KJ, Hayden LJ, Sharma RR, Rocheleau H, Greenberg AH, Edwards DR (1992) Differential regulation of TIMP-1 and TIMP-2 mRNA expression in normal and Ha-ras-transformed murine fibroblasts. Gene 117:209–217

Lindahl GE, Chambers C, Papakrivopoulou J, Dawson SJ, Jacobsen MC, Bishop JE, Laurent GJ (2002) Activation of fibroblast procollagen alpha 1(I) transcription by mechanical strain is transforming growth factor-beta-dependent and involves increased binding of CCAAT-binding factor (CBF/NF-Y) at the proximal promoter. J Biol Chem 277:6153–6161

Lindner V, Wang Q, Conley BA, Friesel RE, Vary CP (2005) Vascular injury induces expression of periostin: implications for vascular cell differentiation and migration. Arterioscler Thromb Vasc Bio 25:77–83

Lluri G, Jaworski DM (2005) Regulation of TIMP-2, MT1-MMP, and MMP-2 expression during C2C12 differentiation. Muscle Nerve 32:492–499

Lovelock JD, Baker AH, Gao F, Dong JF, Bergeron AL, McPheat W, Sivasubramanian N, Mann DL (2005) Heterogeneous effects of tissue inhibitors of matrix metalloproteinases on cardiac fibroblasts. Am J Physiol Heart Circ Physiol 288:461–468

Menko AS, Kreidberg JA, Ryan TT, Van Bockstaele E, Kukuruzinska MA (2001) Loss of alpha3beta1 integrin function results in an altered differentiation program in the mouse submandibular gland. Dev Dyn 220:337–349

Moore KA, Polte T, Huang S, Shi B, Alsberg E, Sunday ME, Ingber DE (2005) Control of basement membrane remodeling and epithelial branching morphogenesis in embryonic lung by Rho and cytoskeletal tension. Dev Dyn 232:268–281

Murphy AN, Unsworth EJ, Stetler-Stevenson WG (1993) Tissue inhibitor of metalloproteinases-2 inhibits bFGF-induced human microvascular endothelial cell proliferation. J Cell Physiol 157:351–358

Ohuchi E, Imai K, Fujii Y, Sato H, Seiki M, Okada Y (1997) Membrane type 1 matrix metalloproteinase digests interstitial collagens and other extracellular matrix macromolecules. J Biol Chem 272:2446–2451

Oshiro W, Lou J, Xing X, Tu Y, Manske PR (2003) Flexor tendon healing in the rat: a histologic and gene expression study. J Hand Surg 28:814–823

Overall CM, Wrana JL, Sodek J (1991) Transcriptional and post-transcriptional regulation of 72-kDa gelatinase/type IV collagenase by transforming growth factor-beta 1 in human fibroblasts. Comparisons with collagenase and tissue inhibitor of matrix metalloproteinase gene expression. J Biol Chem 266: 14064–14071

Rios H, Koushik SV, Wang H, Wang J, Zhou HM, Lindsley A, Rogers R, Chen Z, Maeda M, Kruzynska-Frejtag A, Feng JQ, Conway SJ (2005) Periostin null mice exhibit dwarfism, incisor enamel defects, and an early-onset periodontal disease-like phenotype. Mol Cell Biol 25:11131–11144

Ruwhof C, Wamel AE van, Egas JM, Laarse A van der (2000) Cyclic stretch induces the release of growth promoting factors from cultured neonatal cardiomyocytes and cardiac fibroblasts. Mol Cell Biochem 208:89–98

Sabeh F, Ota I, Holmbeck K, Birkedal-Hansen H, Soloway P, Balbin M, Lopez-Otin C, Shapiro S, Inada M, Krane S, Allen E, Chung D, Weiss SJ (2004) Tumor cell traffic through the extracellular matrix is controlled by the membrane-anchored collagenase MT1-MMP. J Cell Biol 167:769–781

Seeland U, Haeuseler C, Hinrichs R, Rosenkranz S, Pfitzner T, Scharffetter-Kochanek K, Bohm M (2002) Myocardial fibrosis in transforming growth factor-beta(1) (TGF-beta(1)) transgenic mice is associated with inhibition of interstitial collagenase. Eur J Clin Invest 32:295–303

Seiki M (2002) The cell surface: the stage for matrix metalloproteinase regulation of migration. Curr Opin Cell Biol 14:624–632

Seo DW, Li H, Guedez L, Wingfield PT, Diaz T, Salloum R, Wei BY, Stetler-Stevenson WG (2003) TIMP-2 mediated inhibition of angiogenesis: an MMP-independent mechanism. Cell 114:171–180

Skonier J, Bennett K, Rothwell V, Kosowski S, Plowman G, Wallace P, Edelhoff S, Disteche C, Neubauer M, Marquardt H, Rodgers J, Purchio AF (1994) Beta ig-h3: a transforming growth factor-beta-responsive gene encoding a secreted protein that inhibits cell attachment in vitro and suppresses the growth of CHO cells in nude mice. DNA Cell Biol 13:571–584

Skutek M, Griensven M van, Zeichen J, Brauer N, Bosch U (2001) Cyclic mechanical stretching modulates secretion pattern of growth factors in human tendon fibroblasts. Eur J Appl Physiol 86:48–52

Stahl S, Weitzman S, Jones JC (1997) The role of laminin-5 and its receptors in mammary epithelial cell branching morphogenesis. J Cell Sci 110:55–63

Suzuki H, Amizuka N, Kii I, Kawano Y, Nozawa-Inoue K, Suzuki A, Yoshie H, Kudo A, Maeda T (2004) Immunohistochemical localization of periostin in tooth and its surrounding tissues in mouse mandibles during development. Anat Rec 281:1264–1275

Takayama G, Arima K, Kanaji T, Toda S, Tanaka H, Shoji S, McKenzie AN, Nagai H, Hotokebuchi T, Izuhara K (2006) Periostin: a novel component of subepithelial fibrosis of bronchial asthma downstream of IL-4 and IL-13 signals. J Allergy Clin Immunol 118:8–104

Takeshita S, Kikuno R, Tezuka K, Amann E (1993) Osteoblast-specific factor 2: cloning of a putative bone adhesion protein with homology with the insect protein fasciclin I. Biochem J 294: 271–278

Tanabe H, Kii I, Amizuka N, Katsube K, Kudo A (2004) Notch signaling is activated by binding of periostin or CCN3 to Notch1 in osteoblasts. J Bone Miner Res 19:S275

Tsuji K, Uno K, Zhang GX, Tamura M (2004) Periodontal ligament cells under intermittent tensile stress regulate mRNA expression of osteoprotegerin and tissue inhibitor of matrix metalloprotease-1 and -2. J Bone Miner Metab 22:94–103

Wilde J, Yokozeki M, Terai K, Kudo A, Moriyama K (2003) The divergent expression of periostin mRNA in the periodontal ligament during experimental tooth movement. Cell Tissue Res 312:345–351

Yoshiba K, Yoshiba N, Aberdam D, Meneguzzi G, Perrin-Schmitt F, Stoetzel C, Ruch JV, Lesot H (1998a) Expression and localization of laminin-5 subunits during mouse tooth development. Dev Dyn 211:164–176

Yoshiba N, Yoshiba K, Aberdam D, Meneguzzi G, Perrin-Schmitt F, Stoetzel C, Ruch JV, Lesot H (1998b) Expression and localization of laminin-5 subunits in the mouse incisor. Cell Tissue Res 292:143–149

Yoshiba N, Yoshiba K, Stoetzel C, Perrin-Schmitt F, Cam Y, Ruch JV, Lesot H (2003) Temporospatial gene expression and protein localization of matrix metalloproteinases and their inhibitors during mouse molar tooth development. Dev Dyn 228:105–112

Yoshiba N, Yoshiba K, Stoetzel C, Perrin-Schmitt F, Cam Y, Ruch JV, Hosoya A, Ozawa H, Lesot H (2006) Differential regulation of TIMP-1, -2, and -3 mRNA and protein expressions during mouse incisor development. Cell Tissue Res 324:97–104

Yu WH, Yu S, Meng Q, Brew K, Woessner JF Jr (2000) TIMP-3 binds to sulfated glycosaminoglycans of the extracellular matrix. J Biol Chem 275:31226–31232

Zhang W, Ou J, Inagaki Y, Greenwel P, Ramirez F (2000) Synergistic cooperation between Sp1 and Smad3/Smad4 mediates transforming growth factor beta1 stimulation of alpha 2(I)-collagen (COL1A2) transcription. J Biol Chem 275:39237–39245

Differentiation (2007) 75:452–462 DOI: 10.1111/j.1432-0436.2006.00150.x

ORIGINAL ARTICLE

Takashi Yamashiro · Li Zheng · Yuko Shitaku · Masahiro Saito · Takanori Tsubakimoto · Kenji Takada · Teruko Takano-Yamamoto · Irma Thesleff

Wnt10a regulates dentin sialophosphoprotein mRNA expression and possibly links odontoblast differentiation and tooth morphogenesis

Received July 23, 2006; accepted in revised form October 13, 2006

Abstract We have explored the role of Wnt signaling in dentinogenesis of mouse molar teeth. We found that Wnt10a was specifically associated with the differentiation of odontoblasts and that it showed striking colocalization with dentin sialophosphoprotein (Dspp) expression in secretory odontoblasts. Dspp is a tooth specific non-collagenous matrix protein and regulates dentin mineralization. Transient overexpression of Wnt10 in C3H10T1/2, a pluripotent fibroblast cell line induced Dspp mRNA. Interestingly, this induction occurred only when transfected cells were cultured on Matrigel basement membrane extracts. These findings indicated that Wnt10a is an upstream regulatory molecule for Dspp expression, and that cell–matrix interaction is essential for induction of Dspp expression. Furthermore, Wnt10a was specifically expressed in the epithelial signaling centers regulating tooth development, the primary and secondary enamel knots. The spatial and temporal distribution of Wnt10a mRNA demonstrated that the expression shifts from the secondary enamel knots, to the underlying preodontoblasts in the tips of future cusps. The expression patterns and overexpression studies together indicate that Wnt10a is a key molecule for dentinogenesis and that it is associated with the cell–matrix interactions regulating odontoblast differentiation. We conclude that Wnt10a may link the differentiation of odontoblasts and cusp morphogenesis.

Key words odontoblast · Dspp · Wnt10a · dentinogenesis · tooth

Takashi Yamashiro · Yuko Shitaku · Kenji Takada
Department of Orthodontics and Dentofacial Orthopedics
Graduate School of Dentistry
Osaka University, 1-8 Yamadaoka, Suita
Osaka 565-0871, Japan

Takashi Yamashiro (✉) · Li Zheng · Teruko Takano-Yamamoto
Department of Orthodontics and Dentofacial Orthopedics
Graduate School of Medicine and Dentistry
Okayama University, 2-5-1 Shikata-cho
Okayama 700-8558, Japan
Tel: +81 86 2356690
Fax: +81 86 2356694
E-mail: yamataka@md.okayama-u.ac.jp

Takashi Yamashiro · Irma Thesleff
Developmental Biology Programme, Institute of Biotechnology, University of Helsinki, Helsinki 00014, Finland

Masahiro Saito · Takanori Tsubakimoto
Department of Oral Medicine
Division of Operative Dentistry and Endodontics
Kanagawa Dental College
82 Inaoka-cho, Yokosuka
Kanagawa 238-8580, Japan

Introduction

Dentin is one of the three mineralized tissues of the tooth, and it is produced by odontoblasts differentiating from dental papilla mesenchymal cells. Dentin is very similar to bone in its matrix protein composition. However, whereas bone remodels throughout postnatal life and participates in calcium homeostasis, dentin, once formed, does not undergo remodeling. On the other hand, it can respond to injury or stimulation by forming reparative dentin to protect the dental pulp (Linde and Goldberg, 1993). Unlike osteoblast differentiation, the differentiation of odontoblasts is regulated by epithelial–mesenchymal interactions, which instruct both tooth morphogenesis and cell differentiation (Thesleff et al., 1989, 1991; Thesleff and Aberg, 1999). Recombination experiments of the dissociated developing dental

tissues have shown that odontoblast differentiation is controlled by the inner dental epithelium (Ruch et al., 1982; Kollar, 1985; Thesleff et al., 1989). Odontoblasts are columnar polarized cells with eccentric nuclei and long cellular processes, and this cytological polarization specifically occurs in a single cell layer adjacent to the basement membrane of the inner dental epithelium (Linde and Goldberg, 1993). The terminal differentiation of odontoblasts is initiated during the bell stage of tooth morphogenesis at the sites of the future cusps (Lesot et al., 2001; Thesleff et al., 2001). The patterning of the cusps, on the other hand, is determined by the positions of the secondary enamel knots, epithelial signaling centers resembling other embryonic signaling centers, such as the notochord and the apical ectodermal ridge in limbs (Jernvall et al., 1994; Jernvall and Thesleff, 2000). The cells of the enamel knots are non-proliferative, and they express several signaling molecules. These signals may control the folding of the inner enamel epithelium and as odontoblast differentiation starts from the mesenchymal cells underlying enamel knots it has been suggested that signals from the secondary enamel knots may also determine the location and time of the onset of odontoblast terminal differentiation (Thesleff et al., 2001). However the molecular mechanisms of the induction of odontoblast differentiation have remained unknown.

Dentin and bone share many extracellular matrix proteins associated with mineralization such as dentin matrix protein 1, fibronectin, collagen type I, alkaline phosphatase, osteonectin, osteopontin, bone sialoprotein, bono-1, and osteocalcin (Tsukamoto et al., 1992; Nakashima et al., 1994; Shiba et al., 1998; James et al., 2004). Dentin sialophosphoprotein (Dspp) is a non-collagenous extracellular matrix protein that is specifically expressed by odontoblasts (D'Souza et al., 1997). Dspp is a phosphorylated parent protein that is cleaved post-translationally into two proteins: dentin sialoprotein (Dsp) and dentin phosphoprotein (Dpp) (Feng et al., 1998). *In situ* hybridization and other experimental analyses have shown that *Dspp* is expressed predominantly in odontoblasts, transiently in preameloblasts, and at low levels in osteoblasts (D'Souza et al., 1997; Qin et al., 2002). In humans, several mutations have been identified in patients with dentinogenesis imperfecta, which is an autosomal dominant disorder of the tooth that specifically affects dentin biomineralization (Shields et al., 1973; Xiao et al., 2001; Zhang et al., 2001; Rajpar et al., 2002). A similar phenotype is found in *Dspp* null mutant mice, which feature a disturbance of dentin mineralization without any influences on bone (Sreenath et al., 2003). Hence, it is established that Dspp has a crucial role in the formation of mineralized dentin. Although the importance of epithelial–mesenchymal interactions and extracellular matrix for odontoblast differentiation is established, the molecular mechanisms of the interactions mediating odontoblast differentiation and inducing *Dspp* expression are not known.

Wnt genes encode a large family of secreted signaling proteins that specify various cell lineage pathways in development. Wnt proteins are now recognized as one of the major families of developmentally important signaling molecules and they regulate such intriguing processes as embryonic induction, the generation of cell polarity, and the specification of cell fate (Cadigan and Nusse, 1997; Nusse, 2003). In early tooth development, several Wnt genes are expressed from the initiation stage to the early bell stage (Sarkar and Sharpe, 1999). Targeted inactivation of lymphoid enhancer factor-1 (LEF1), a nuclear mediator of Wnt signaling, results in an arrest of tooth development at the bud stage (van Genderen et al., 1994). LEF1 serves as a relay of a Wnt signal to a fibroblast growth factor signal in the enamel knot in the dental epithelium, which establishes a network of reciprocal and sequential signaling between epithelium and mesenchyme (Kratochwil et al., 2002).

Here we provide evidence that Wnt10a signaling may be involved in odontoblast terminal differentiation, and based on the expression pattern of *Wnt10a*, we suggest that it has a role in linking tooth morphogenesis and odontoblast differentiation.

Materials and methods

Materials

Lipofectamine Plus was obtained from Gibco BRL (Gaithersburg, MD). Biocoat Matrigel-coated dishes were from Becton Dickinson (Labware, MA). The rabbit polyclonal anti-Wnt10a antibody was produced by Sigma Genosys Co. (Hokkaido, Japan) using a synthetic peptide as antigen, which was established by the Wnt10a protein sequence analysis (U61969). The amino acid sequence of the antigen peptide is RRGDEEAFRRKLHR and corresponds to amino acids 163–176 of the Wnt10a protein. All other chemicals were analytical grade.

Processing of tissues

Wild-type mouse embryos were obtained from the NMRI strain. Heads of embryonic E12, E13, E14, and E16 mice and postnatal 14 day old mice were dissected in Dulbecco's phosphate-buffered saline. The tissues were fixed in 4% paraformaldehyde at 4°C overnight. P14 heads were decalcified in 12.5% ethylene-diamine-tetra-acetic acid (EDTA) for 3 weeks. They were dehydrated, embedded in paraffin and serially sectioned at 7 μm.

Probes and *in situ* hybridization

The mouse *Wnt10a* cDNA was kindly provided by Dr Andrew P. McMahon, Harvard University, Boston, MA. Mouse *Dspp* probes were generated from A 550 bp *Dspp* fragment spanning the region between 656 and 1205 in accession # NM010080. The preparation of Bmp3 RNA probes has previously been described (Åberg et al., 1997). *In situ* hybridization of paraffin sections using 35S-UTP-labeled riboprobe was performed as described previously (Vainio

et al., 1993). The bright field and dark field images of each section were digitized, and the grains from dark fields were selected, colored red, and added to the bright field pictures in PhotoShop 6 (Åberg et al., 1997). Keratin was used as a marker for epithelial cells and it was detected by immunohistochemistry using polyclonal pan-keratin antibodies (DAKO, A575, Glostrup, Denmark) (Yamashiro et al., 2003).

Cell cultures

C3T10T1/2 cell lines, derived from embryonic mouse mesenchyme, were obtained from Riken cell bank (Tsukuba, Japan). These cells were cultured in Dulbecco's modified Eagle's medium (D-MEM, high glucose (4,500 mg/l D-glucose), with L-glutamine, and phenol red) supplemented with 0.1 mM non-essential amino acids (NEAA), 10% fetal bovine serum (FBS), 100 units U/ml penicillin, 100 µg/ml streptomycin, and incubated at 37°C in a 5% carbon dioxide, 95% air, humidified atmosphere. The cells were subcultured every 3–4 days, using 0.05% (w/v) EDTA to detach cells from the culture dish.

Wnt10a transfection in C3T10T1/2 cells

Mammalian expression vectors encoding mouse Wnt10 were constructed for transient transfections. Full-length mouse *Wnt10a* cDNA (Wang and Shackleford, 1996), pj32 was kindly provided by Dr. Gregory M. Shackleford, University of Southern California, Los Angeles, CA. *Wnt10a* was transferred from pj32 to the multiple cloning site of pCMV-Script (Stratagene, La Jolla, CA) with the restriction sites *Eco*RI and *Xho*I to generate pCMV-Wnt10a. Cells (60%–80% confluence) were transiently transfected with Lipofectamine Plus reagent (Gibco BRL, Gaithersburg, MD) according to the manufacturer's instructions. Briefly, pCMV-Wnt10a was mixed with Plus reagent in Opti-MEM I and incubated at room temperature for 15 min. Lipofectamine was mixed with DNA plus reagent and incubated further at room temperature for 15 min. Then the Lipofectamine Plus cDNA complex was added to the cells and incubated at 37°C. The control cells received Lipofectamine Plus alone. After 5 hr of incubation, growth medium containing 20% FBS was added for a final concentration of 10% FBS. The cells were maintained for an additional 12 hr. One day after transfection, cells were plated on Matrigel-coated dishes (Biocoat, Becton Dickinson Labware, Bedford, MA) or conventional culture dishes (Falcon, Becton Dickinson Labware).

Western blot analysis of Wnt10a

Cell lysate proteins (10 µg) from transfected cells were separated using 7.5% sodium dodecyl sulfate-polyacrylamide gel electrophoresis (SDS-PAGE) and were electrophoretically transferred from gel to polyvinylidene difluoride membranes. To separate non-specific protein binding, the membranes were incubated in 10 mM Tris HCl, pH 7.5, 100 mM NaCl, and 0.1% Tween 20 (TBST) containing 3% blot-qualified bovine serum albumin for 1 hr. The membranes were incubated in TBST containing a 1:1,000 diluted anti-Wnt10a antibody (Sigma Genosys Co, Hokkaido, Japan). Wnt10a polyclonal rabbit antibody was produced by Sigma Genosys Co based on the Wnt10a sequence CRRGDEEAFRR KLHR. Wnt10a antibody recognizes a band of approximately 48 kDa that corresponds to the size of Wnt10a in Wnt10a-transfected cells, while mock-transfected cells gave no signal (Fig. 2B). This signal disappeared after preincubation of the antibody with excess antigenic peptide CRRGDEEAFRRKLHR indicating that the band is specific.

The membrane was washed twice for 15 min each with 0.1% TBST, and incubated for 45 min with the secondary antibody, horseradish peroxidase (HRP)Rabbit-conjugated goat anti-rabbit (Amersham, Amersham, UK). Bound antibodies were visualized by chemiluminescence using an ECL Western Immunoblotting Kit (Amersham).

Reverse-transcriptase polymerase chain reaction (RT-PCR) of *Dspp* and *Wnt10a*

To determine whether *Wnt10a* overexpression in C3H10T1/2 cells induces *Dspp* expression, real-time PCR amplification of *Dspp* was performed. Five, ten and fifteen days after transfection, total RNA was isolated using the RNeasy-kit (Qiagen, Valencia, CA) according to the manufacturer's instructions. First molar tooth germs of the mandible from day 1 postnatal mouse pups were dissected in Dulbecco's PBS under a stereomicroscope. Total RNA was also isolated from tooth germs using the RNeasy-kit (Qiagen). Total RNA (1 µg) was reverse transcribed in 20 µl of transcription buffer [75 mM KCl, 50 mM Tris/HCl pH 8.3, 10 mM dithiothreitol, 3 mM $MgCl_2$, 0.5 mM deoxyribonucleotide trisphosphate, 1 µg oligo(dT)18-adapter primer] with Superscript II reverse transcriptase (200 U) for 1 hr at 42°C. Presence of *Dspp* and *Wnt10a* mRNA was determined using the LightCycler System and the Faststart DNA Master SYBR Green I kit (both from Roche Diagnostics, Mannheim, Germany). PCRs were performed according to the manufacturer's instructions with 0.5 µm each of the respective forward and reverse primers, 4 mM $MgCl_2$, and 1 × Faststart DNA Master SYBR Green I mix in a total volume of 20 µl. Cycling conditions were as follows: 10 min at 94°C, followed by 40 cycles with 15 sec C at 94°C, 10 sec at 64°C and 45 sec at 72°C. Standard GAPDH RT-PCR was used as an internal control for an adequate PCR reaction (472 bp). The following primers were used: 5′-atagcaccaaccatgag gct-3′ and 5′-cttttgttgcctttgttggg-3′ for *Dspp* gene, 5′-aactttggcattgt ggaagg-3′ and 5′-ggtcctcagtgtagcccaag-3′ for *Wnt10a*, 5′-aactttggc attgtggaagg -3′ and 5′-ccctgttgctgtagccgtat-3′ for GAPDH gene. PCR primer set for Dspp was designed for controlling the genomic DNA contamination. Primers that span intron–exon boundaries amplify a product from contaminating DNA that includes the intron, making it larger than the expected cDNA product. The products from the reactions described above were also run on a 1% (w/v) agarose gel, to confirm that all products were of the correct length for the primers used. After amplification, melting curve analysis of the PCR product was used to differentiate between specific and non-specific amplification products. Melting curve was acquired by heating the product at 20°C/sec to 95°C, cooling it at 20°C/sec to 55°C for 30 sec, and slowly heating it at 0.1 µC/sec to 94°C under continuous fluorescence monitoring. Melting curve analysis was accomplished with LightCycler software.

Results

Expression of *Wnt10a* and *Dspp* in the developing root

We evaluated the mRNA expression of several Wnt genes during root development at postnatal day 14, and found that *Wnt10a* transcripts were specifically present in the dental mesenchymal cells lining the inner dentin surface (Fig. 1A). *Dspp* mRNA was specifically expressed in odontoblasts (Fig. 1B), as shown previously (D'Souza et al., 1997; Bleicher et al., 1999), and both *Wnt10a* and *Dspp* were absent in the dental papilla cells, osteoblasts and cementoblasts.

The epithelial root sheath is a two-cell layer sheet at the apical end of the growing root and it regulates root growth as well as odontoblast differentiation. The root sheath can be visualized by immunohistochemistry

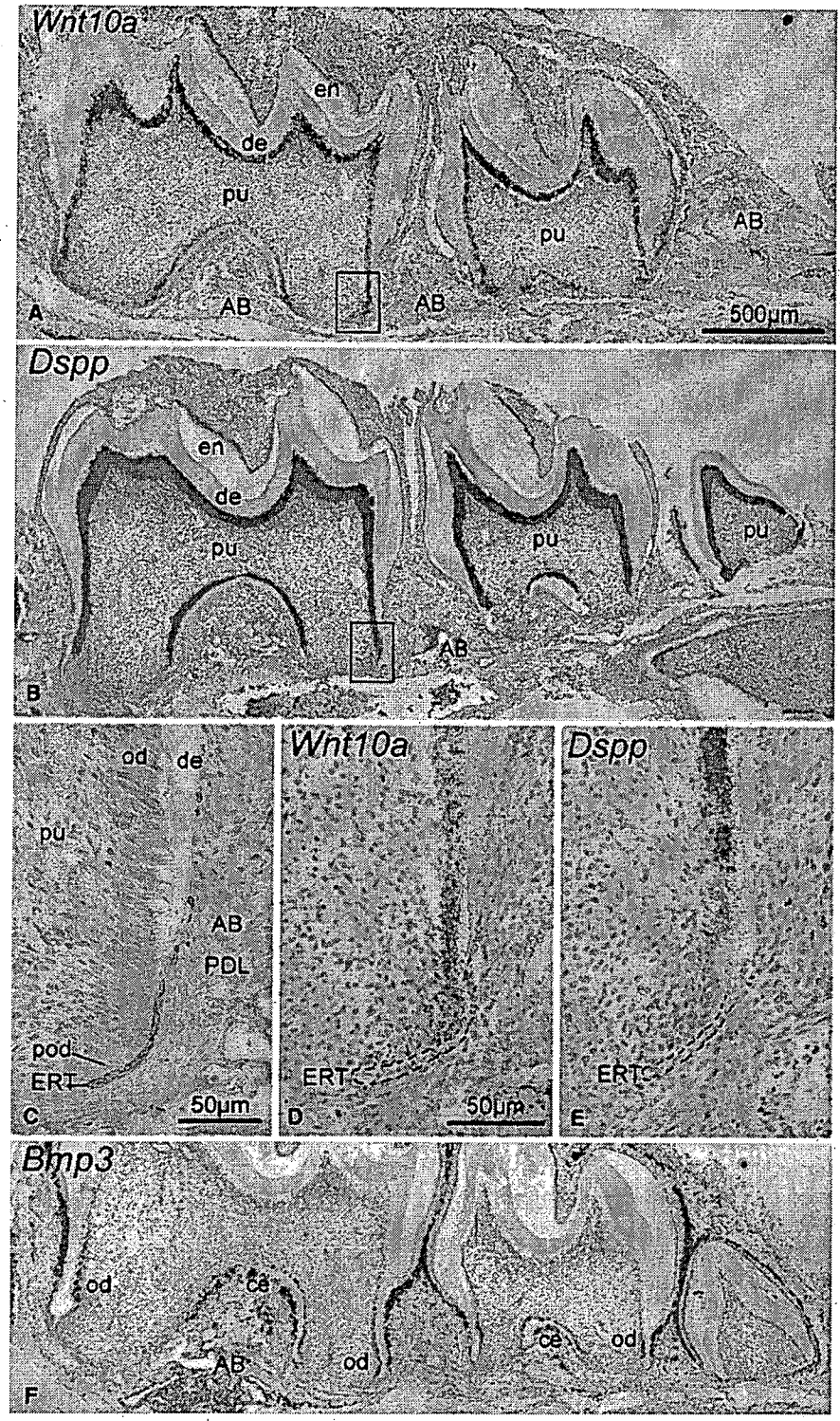

Fig. 1 Wnt10a and Dspp mRNA expression in lower jaw sections of a 14-days-old mouse (**A**, **B**) *Wnt10a* transcripts were specifically present in the odontoblasts lining the dentin (de) surface but not in the dental papilla cells (pu), or osteoblasts in the alveolar bone (AB). *Dspp* transcripts were also specifically present in odontoblasts. In higher magnification, the epithelial root sheath (ERT) is localized by immunohistochemistry using pan-keratin antibodies. Odontoblasts (od) are columnar cells lining the pulpal surface of dentin (de), and preodontoblasts (pod) are the odontoblast precursors in the apical end of the root. At the apical end of the growing root, *Wnt10a* transcripts were present in the preodontoblasts (pod). (**D**) The expression was continuous and maintained in differentiating and secretory odontoblasts (od). (**E**) *Dspp* expression was only detected in polarized odontoblasts (od). en, enamel; PDL, periodontal ligament. (**F**) Strong *Bmp3* expression was detected in cementoblasts the 1st and 2nd molars, as well as the dental follicle around all three molars. It was also observed in the osteoblasts on the active bone-forming surface.

using pan-keratin antibodies (Fig. 1C). Odontoblasts can be visualized as columnar cells lining the pulpal surface of dentin, and as the gradient of cell differentiation extends towards the root apex, preodontoblasts, i.e. the odontoblast precursors are present next to the root sheath (Fig. 1C). In higher magnification, *Wnt10a* transcripts were detected in differentiating and secretory odontoblasts and they were also diffusely present in the preodontoblasts underlying the epithelial root sheath (Fig. 1D). Previous reports showed that *Dspp* expres-

sion is initiated with matrix mineralization. *Dspp* was present in polarized odontoblasts but absent in pre-odontoblasts and differentiating odontoblasts indicating that the expression of *Wnt10a* precedes *Dspp* during the differentiation of the odontoblast cell lineage (Fig. 1E). At this stage, osteogenesis and cementogenesis were also active, as shown by intense *Bmp3* signals on the surfaces of bone and cementum (Fig. 1F) (Yamashiro et al., 2002). Hence, *Wnt10a* expression was expressed specifically in secretory odontoblasts

Wnt10a overexpression induces *Dspp* expression

As *Wnt10a* and *Dspp* transcripts overlapped in the odontoblasts but *Wnt10a* appeared earlier than *Dspp* in the odontoblast cell lineage, we hypothesized that Dspp might be induced by Wnt10a. To test this possibility, we overexpressed *Wnt10a* in the C310T1/2 cell line and examined its effect on *Dspp* expression. RT-PCR confirmed that C310T1/2 cells and Mock-transfected cells did not express *Wnt10a* mRNA, whereas *Wnt10a* transfected cells at 24 hr post-transfection and the cells derived from P1 tooth germs showed 340-bp bands of *Wnt10a* (Fig. 2A).

Induction of *Dspp* expression was detected in the *Wnt10a* transfected cells by real-time PCR ten days after transfection, but not after five or fifteen days. C3H10T1/2 cells did not show *Dspp* expression (Figs. 3A,3B). Gel electrophoresis of RT-PCR products (40 cycles) demonstrate a single band of 550 bp, corresponding to the *Dspp* transcript in cDNA derived from total RNA obtained from C310T1/2 cells transfected with pCMV-Wnt10a and cultured on Matrigel (Wnt10a Mg(+)), and positive control (tooth germ; Fig. 3B), indicating that *Dspp* induction was seen only when the cells were cultured on Matrigel coated dishes. Matrigel is an extract of basement membrane proteins (Kleinman et al., 1982 #16), and *Wnt10a* transfected cells cultured on conventional collagen coated dishes did not express *Dspp*. Mock transfected cells cultured on Matrigel dishes did not show *Dspp* expression (Figs. 3A,3B), indicating that Matrigel itself did not induce *Dspp*. These results indicated that Wnt10 can induce *Dspp* expression and that the specific basement membrane matrix was essential for this induction.

We confirmed the specificity of the amplified products and PCR products were not detected in Mock-transfected cells. The integrity of the RT-PCR products was confirmed by melting curve analysis (Fig. 3C). Melting curve analysis showed that the Tm of the *Dspp* templates was 88.5°C and occurred as a single amplicon peak for both *Wnt10a* transfected cells and control samples, reflecting the specificity of the PCR-products (Fig. 3C). The non-specific products, such as primer dimers, sometimes appeared, however, they melt below 80°C and were differentiated from the specific products by the melting curve analysis. These results were also confirmed by gel electrophoresis. Transfection and PCR were repeated three times.

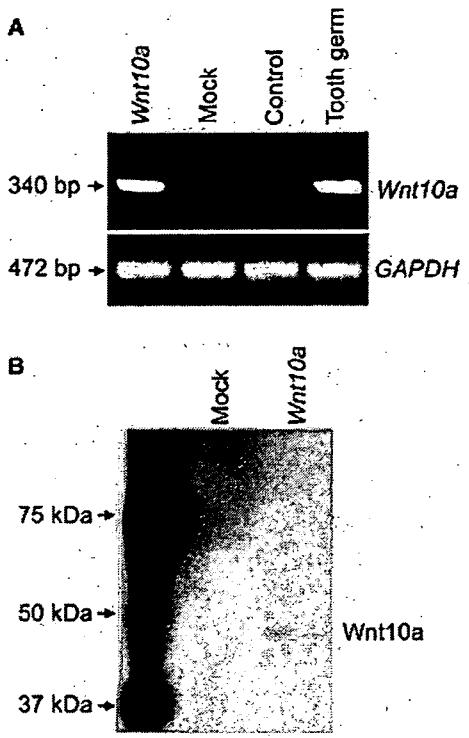

Fig. 2 C310T1/2 cells were transiently transfected with expression vectors encoding *Wnt10a*. (A) Expression of *Wnt10a* mRNA in C310T1/2 cells. After 24 hr transient transfection, total mRNA was extracted and submitted to reverse-transcriptase polymerase chain reaction (RT-PCR) using oligonucleotide primers specific of *Wnt10a* and *GAPDH*. Cells were transfected with pCMV-Wnt10a (Wnt10a) or its vehicle pCMV (Mock). Total RNA was also isolated from tooth germs and used as a positive control (tooth germ, 30 cycles). Negative control (control, 30 cycles) was performed in the absence of oligonucleotides. RT-PCR confirmed transfection efficiency using pCMV-WNT10a (Wnt10a, 30 cycles). (B) Expression of Wnt10a protein in C310T1/2 cells. Overexpression of Wnt10a protein was also confirmed by Western blot analysis 48 hr after transfection. Cells were lysed in sodium dodecyl sulfate-polyacrylamide gel electrophoresis (SDS-PAGE) loading buffer after transfection and analyzed by Western blot with specific antibodies to Wnt10a. pCMV-Wnt10-transfected (Wnt10a) cells showed Wnt10a protein expression. This protein expression was not observed in control cells transfected with vehicle pCMV (Mock). A molecular weight marker was run in parallel in the first lane.

Expression of *Wnt10a* during tooth development

At E14, the cap stage of tooth development, *Wnt10a* transcripts were intensely expressed in the enamel knot, as shown previously (Dassule and McMahon, 1998). No *Wnt10a* expression was detected in the dental mesenchyme (Fig. 4A). At E16, early bell stage, the primary enamel knot had disappeared, and *Wnt10a* was detected in secondary enamel knots. In addition, the mesenchymal cells directly underlying the enamel knots expressed *Wnt10a* (Fig. 4B). Subsequently at E18 transcripts were

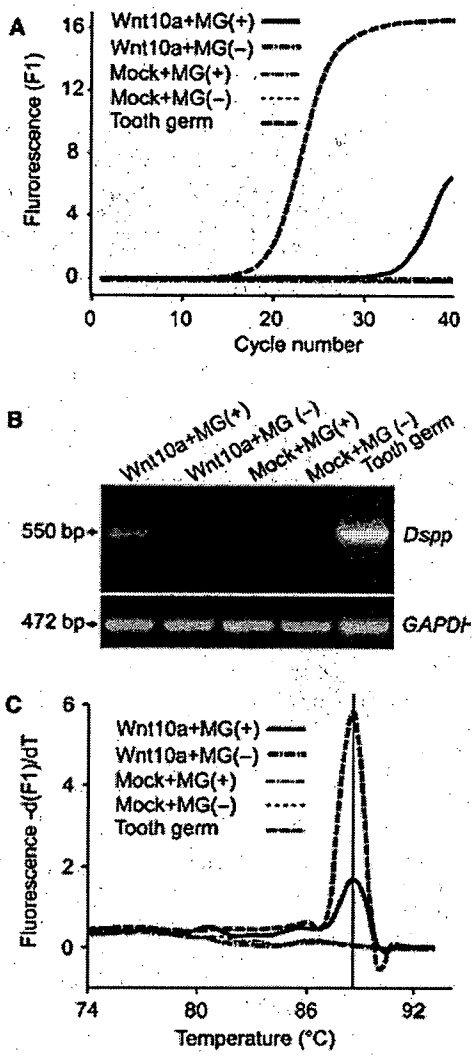

Fig. 3 Wnt10a transient transfection in C310T1/2 cells induced dentin sialophosphoprotein (Dspp) gene expression. (A) C310T1/2 cells were transiently transfected with pCMV-Wnt10a (Wnt10a) or its vehicle pCMV (Mock). Transfected cells were harvested 10 day post-transfection on Matrigel (Mg (+)) or collagen coated dishes (Mg (−)). Total mRNA extracted from the transfected cells was reverse transcribed and submitted to real-time polymerase chain reaction (PCR) using oligonucleotide primers specific of Dspp. Total RNA was also isolated from tooth germs and used as a positive control (Tooth germ). The *x*-axis denotes the cycle number of a quantitative PCR assay, and the y axis denotes the fluorescence intensity (F1) over the background. Amplification of Dspp was observed in C310T1/2 cells transfected with pCMV-Wnt10a and cultured on Matrigel (Wnt10a+Mg (+)), and positive control (tooth germ). (B) Forced-expression of Wnt10a induced Dspp expression when the transfected cells were cultured on Matrigel dishes (Wnt10a+Mg (+), 40 cycles). Wnt10a transfected cells cultured on normal culture dishes (Wnt10a+Mg (−), 40 cycles) and Mock transfected cells cultured on Matrigel dishes (Mock+Mg (+), 40 cycles) or normal culture dishes (Mock+Mg (−), 40 cycles) did not show Dspp expression. Positive control (Tooth germ) showed intense Dspp expression. (C) PCR products were subjected to melting peak analyses to determine the specificity of the products. Dspp sample showed a single product with Tm values of 88.5°C.

accumulated in the single cell layer of differentiating odontoblasts, which were aligned under the basement membrane (Fig. 4C). At E18, the differentiating odontoblasts became polarized and odontoblast differentiation initiated from the tips of the future cusps where the enamel knots are located (Fig. 5A). As the differentiation of preodontoblasts proceeded from the cusp tips in cervical direction along the cusp slopes *Wnt10a* expression was intimately linked with this gradient of differentiation. (Fig. 5B), and was highest in the cusp regions (Fig. 5C). *Dspp* expression was not yet expressed in the odontoblast lineage at this stage (Bleicher et al., 1999). In the early osteogenesis, *Wnt10a* was detected in the future bone regions at E13 and E14 (data not shown). This expression was down-regulated significantly at E16 and the expression could not be detected at P14 (Fig. 1A).

Discussion

The expression pattern of *Wnt10a* is associated with odontoblast differentiation

Our *in situ* hybridization analysis revealed that the expression of *Wnt10a* mRNA was associated with dentinogenesis. We found that *Wnt10a* expression was intense in the odontoblast cell layer and that it was maintained specifically in secretory odontoblasts where it was coexpressed with *Dspp*. In root development stage, mineralized matrix is also actively formed on the surface of bone and cementum, and the distribution of *Bmp3* expression indicated the regions of active osteogenesis and cementogenesis at the root surface and the surrounding alveolar bone surface. The comparison of *Wnt10a* and *Bmp3* distribution revealed that *Wnt10a* expression was specifically involved in odontogenesis, but not in osteogenesis or cementogenesis.

At the tip of the growing root, Hertwig's epithelial root sheath proliferates and directs root morphogenesis. The pulpal mesenchyme provides precursors for odontoblasts, and the subpopulation of pulp cells that contact the epithelial root sheath differentiate into preodontoblasts. As odontoblast differentiation is characterized by cytological polarization and they are lining in one cell layer they can be clearly distinguished from the surrounding pulpal cells. *In situ* hybridization analysis demonstrated that *Wnt10a* was not expressed in the pulpal mesenchyme, indicating that Wnt10a is induced when the precursor cells start to differentiate into odontoblasts.

Wnt10a regulates the expression of *Dspp*

Dspp and *Wnt10a* were colocalized in the differentiated odontoblasts. However, at the tip of the growing root,

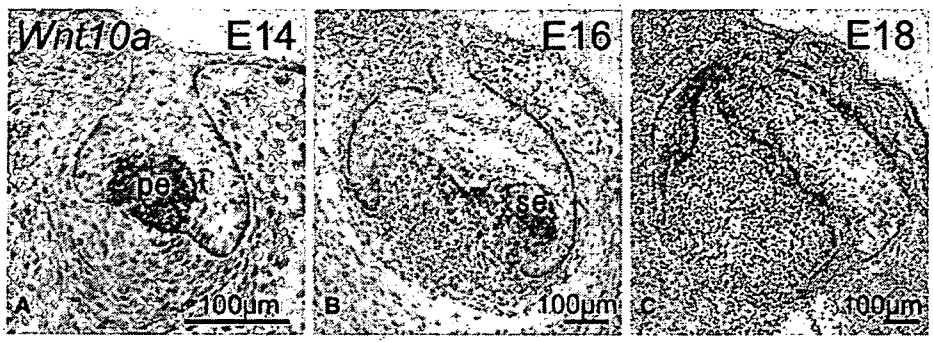

Fig. 4 At E14 (cap stage) *Wnt10a* transcripts were present in the primary enamel knot (pe), as shown previously. No expression was detected in the dental mesenchyme (A). At E16 (early bell stage) *Wnt10a* was detected in secondary enamel knots (se). In addition gene expression had shifted to the underlying mesenchymal cells (B). At E18 transcripts were accumulated in the single cell layer of differentiating odontoblasts (C).

Wnt10a expression was present in preodontoblasts beneath the epithelial sheath, but *Dspp* expression was absent indicating that *Wnt10a* expression appeared earlier than *Dspp* expression. Similarly, in early tooth development *Wnt10a* expression was first initiated in the odontogenic lineage cells at E14 whereas *Dspp* appeared in odontoblasts at E17 (Yamazaki et al., 1999). This temporo-spatial distribution pattern was in line with the possibility of an inductive role of *Wnt10a* on *Dspp* expression and we confirmed by transient overexpression of *Wnt10a* in C310T1/2 cells that Dspp was downstream of Wnt10a. The C310T1/2 cell line is derived from embryonic mesodermal cells, and can differentiate into distinctly different cell lineages, myoblasts, adipocytes, chondrocytes and osteoblasts under the influence of certain inducers (Taylor and Jones, 1979; Katagiri et al., 1990; Asahina et al., 1996). As C31010T1/2 cells did not constitutively express either *Wnt10a* or *Dspp* mRNA, our data indicated that *Dspp* was induced by Wnt10a in C31010T1/2 cells and that it may be a direct downstream target of Wnt10a (Fig. 6).

The extracellular mineralizing matrices of dentin and bone share many similarities, and it is likely that regulation of osteoblast and odontoblast differentiation may involve same signaling molecules (Thesleff et al., 2001). To our knowledge, Wnt10a is the first signal molecule that has specifically associated with odontoblast differentiation. Various Wnt genes, such as *Wnt1*, *Wnt4*, *Wnt5a*, *Wnt9a/14* and *Wnt7b*, are expressed in either osteoblast precursors or adjacent tissues during embryonic development, and *Wnt3a* and *Wnt10b* are expressed in bone marrow (Hartmann, 2006). In our study, we also demonstrated that *Wnt10a* was expressed in the future bone regions, but its expression was not maintained in the postnatal bone. Among these Wnt molecules, *Wnt10b* mutants display a postnatal decrease in bone mass and serum osteocalcin level, indicating that Wnt10b is an endogenous regulator of bone formation (Bennett et al., 2005). Wnt10b is homologous to Wnt10a, and WNT6 and WNT10a genes are clustered in tail-to-head manner. Like *Wnt10a*, both *Wnt10b* and *Wnt6* are expressed in the enamel knot and the dental epithelium in early tooth development (Dassule and McMahon, 1998; Sarkar and Sharpe, 1999). However, during later tooth development, *Wnt6* or *Wnt10b* transcripts were not detected in the odontoblast cell lineage by *in situ* hybridization (data not shown).

Cell to matrix interactions are required for the induction of *Dspp* expression by Wnta10a

Studies in the 1970's and 1980's showed that odontoblast differentiation depends on contacts between the

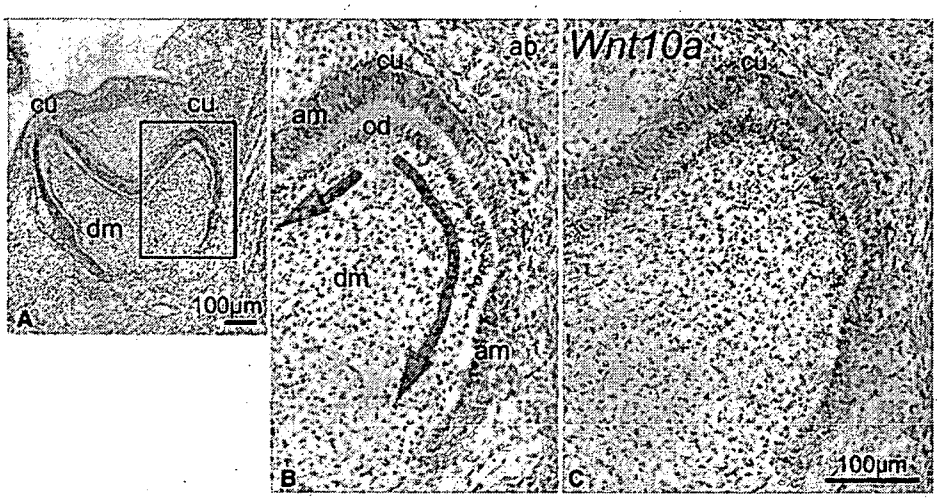

Fig. 5 Coronal sections of E18 molar (late bell stage) (A). (B) Higher magnification of the labial half of 1st molar (inset in panel A). Odontoblast differentiation has initiated beneath the forming cusp (cu) and the cells have polarized. (C). Wnt10a expression is associated with the gradient of odontoblast cytodifferentiation, and is highest in the cusp regions (cu).